STRUCTURAL GEOLOGY AND TECTONIC GEOMORPHOLOGY OF THE NORTHEASTERN CAUCA-AMAGÁ VALLEY BASIN, NORTHERN ANDES BLOCK: EVIDENCE OF NEOTECTONICS ALONG THE CAUCA-ROMERAL FAULT SYSTEM

Final work to apply for the

Geology degree

by

Escobar-Monsalve, Santiago
201310036015 sescob39@eafit.edu.co

Mesa-Escobar, Simón
201410023015 smesaes2@eafit.edu.co

Universidad EAFIT
Escuela De Ciencias.
(050021) Carrera 49 N° 7 Sur-50
Colombia

STRUCTURAL GEOLOGY AND TECTONIC GEOMORPHOLOGY OF THE NORTHEASTERN CAUCA-AMAGÁ VALLEY BASIN, NORTHERN ANDES BLOCK: EVIDENCE OF NEOTECTONICS ALONG THE CAUCA-ROMERAL FAULT SYSTEM

Authors
Escobar-Monsalve, Santiago
201310036015 sescob39@eafit.edu.co
Mesa-Escobar, Simón
201410023015 smesaes2@eafit.edu.co

Director
Beltrán-Triviño, Alejandro, Professor Dr.
aibeltrant@eafit.edu.co.

Universidad EAFIT
Escuela De Ciencias.
(050021) Carrera 49 N° 7 Sur-50
Colombia

Abstract:

We disclose new evidence of neotectonic activity associated with the Romeral fault system in the western flank of the Central Cordillera of the Colombian Andes and, provide a geomorphological analysis of a dynamic fluvial system related to this structural setting. This region is populated by several large cities and has been attached to a recent history of natural disasters such as the 1999 Armenia earthquake, therefore the effort to understand relative timing and surface expression of neotectonic events is more than worth. We use an integrated approach of structural geology and tectonic geomorphology to understand the relationship between geomorphic markers and active faults and other controls of landscape evolution such as denudation and fluvial agents. We propose that neotectonics in the study area is caused by triple-point stress within a transpressive kinematic model, that produced compressive and distension stress tensor along the Arma fluvial system and a clockwise motion on the western structural blocks.

Keywords: Cauca-Amagá basin, North Andes, Morpho-neotectonics, paleo-stress, geomorphology, Arma river.

This research did not receive any specific grant from funding agencies in the public, commercial, or not-for-profit sectors.

1. Introduction

Morpho-neotectonics research focuses on the relationships between landforms and earth surface modification types; brought about by recent tectonic pulses that produced direct types such as earthquakes cracks and landslide phenomena; or indirect types such as scarps, asymmetrical valleys and river bend. The study of geomorphological effects, both direct and indirect, may lead back to the neotectonic movements that produced them and enable to estimate the chance of recurrence in the future. (Carraro, 1976; Panizza and Piacente 1978; Panizza, 1983; in Panizza and Castaldini, et al., 1987)

The Arma river region in the western flank of the Central Cordillera (Fig. 1) offers a great opportunity to study the relationship between landforms and earth surface dynamics. The local geology exhibits complex lithology interactions between the Cajamarca complex (Paleozoic) and Cambumbia Stock (Triassic), Quebradagrande complex (Cretaceous), Amagá Fm (Paleogene), and Combia Fm (Neogene) and most importantly, regional fault structures (e.g. Calle, et al. 2009; Gonzales, et al 2009). The relationships between denudational, fluvial and tectonic geomorphology processes model and preserve evidence of tectonic activity, such as triangular facets, structural ridges, knickpoints, among others. However, the neotectonic evidence still is not enough to conclude a recent dynamic behaviour of the Cauca valley, because

of the gap on timing and a poor amount of neotectonic studies in the Cauca-Amagá and Cauca-Santa Fe de Antioquia valleys, where large populated centres are located.

The Cauca-Amagá valley evolves from a passive margin (Permian-Jurassic) to a pull-apart basin (Cretaceous-Early Paleocene), finally, a push-up basin (Middle Paleocene- Neogene), controlled by the Romeral fault System (Bustamante et al. 2016; Vinasco and Cordani, 2012). The last ENE-WSW Nazca plate subduction reactivates the sinistral NW-SE Arma fault and the sinistral-reverse N-S Romeral fault System; also controlling NE-SW alignments related to a Western Cordillera dextral fault system (Peláez, 2016).

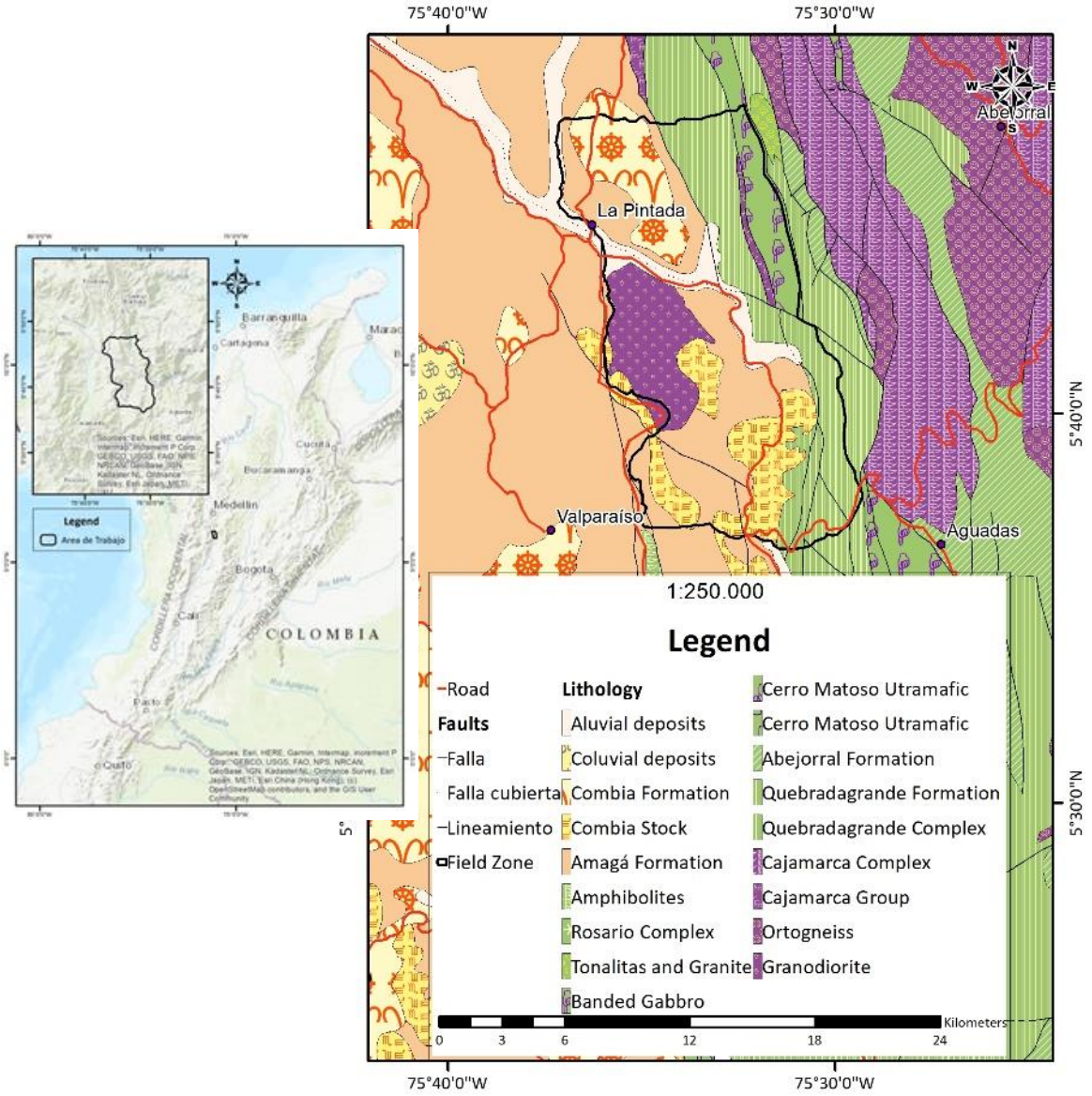

Figure 1. Localization map of the study area. Left) Map of the western part of Colombia showing main cities and localization of the studied area. Right) Geological Map of the studied area (modified from SGC, 2015).

To find evidence to determine if this area has been affected by tectonics in the recent time (Holocene) and to establish the stress tensor on the zone of study, the methods focus on joint and paleo-stress tensor analysis and a denudational, tectonic and fluvial geomorphologic mapping, along with the identification of the Arma river knickpoints, channel patterns and terrace deposits. This research aims to relate the geomorphology and kinematic evidence to establish possible neotectonics indicators. We show that the tectonics environment of the northeastern part of the Cauca-Amagá valley developed under a transpressive kinematic, that produced compressive and distension stress tensor along the Arma fluvial system.

2. Geological setting

The Central Colombian Cordillera mostly includes continental, and oceanic volcanic arcs related to the Pangea dissembling occurred during the Permian to the Early Cretaceous passive oblique margin, which was generally metamorphosed into schist to gneiss facies and later intruded by Jurassic to Paleogene plutonic rock complexes (Spikings, et al. 2015). The Western flank of the central cordillera is composed by the Jurassic-Cretaceous Cajamarca and Arquía complexes, the Early to middle Cretaceous un-metamorphosed tholeiitic complexes as Quebradagrande complex and the Cretaceous to Neogene volcanic and plutonic complexes as Combia Volcanic and Stock (Fig. 1.b) (Bustamante et al. 2016; Nivia et al. 2006; Quintero et al. 2014).

The Northwestern part of the South American plate (Fig. 2) is divided on Choco-Panama, North Andes and Maracaibo blocks, subducted by Nazca plate which is divided on Carneige Ridge (during Miocene) between North-Ecuador and south Colombia; the Malpelo Ridge over Cali's latitude and Coiba Ridge over Choco-Panama Block (both during Pliocene to recent) (Suter, et al. 2008). Despite, Carbon 14 dating over western foothill colluvial-alluvial deposits of the Central Cordillera determine a range of seismic episodes over the last 22 ka (Salcedo, et al. 2017; Suter, et al. 2011). The Cauca valley has 3 basins the Cauca-Quindío-Risaralda, Cauca-Amagá and Cauca-Santa Fe de Antioquia valleys, where two tectonic environments control the stress propagation, middle cortical faults (~64 km deep) with 130 cm fault displacement and superficial faults (~32 km deep) with 65 cm fault displacement (Salcedo, et al. 2017).

2.1. Jurassic to Cretaceous

Geological and geochronological data from the Central Cordillera indicate the existence of Late Triassic to Late Jurassic magmatism between 203 and 145 Ma (Bustamante et al. 2016), these are caused by the presence of a stationary arc that occasioned magmatic quantity, as a consequence of oblique plate convergence between the Farallon plate and the South America

plate, triggered a long-term evolution of the magma sources. During this evolution, two subduction collision and accretion events caused metamorphism during Permian to Triassic and Middle to Late Cretaceous (Vinasco, 2019). The metamorphism age was described as Permian, but later defined as Middle to Late Triassic between 240 and 230 Ma; associated with syntectonic S-type granites based on the crystallization age of spatially and 40Ar-39Ar amphibole cooling ages (Quintero et al. 2014).

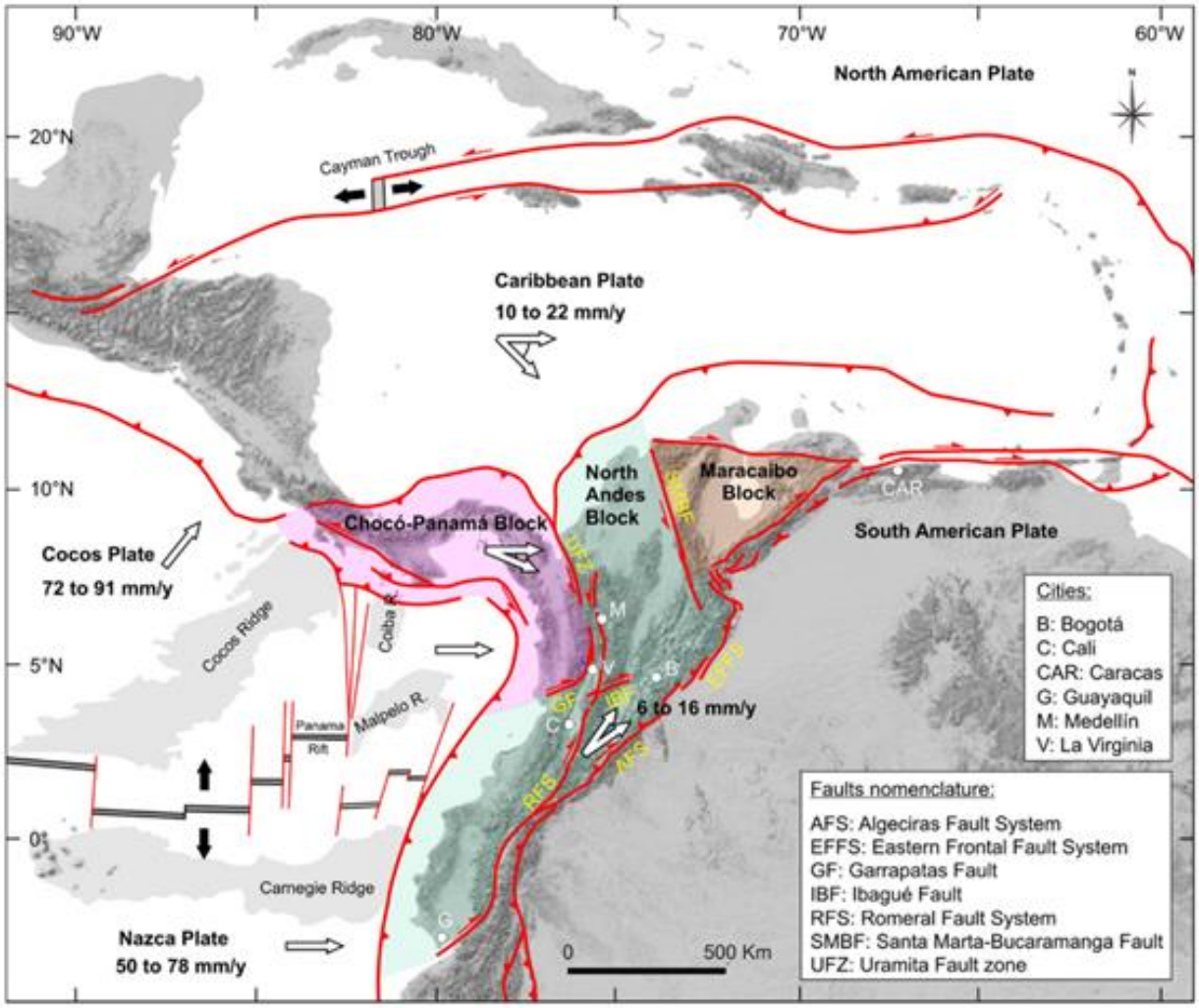

Figure 2. NW Geodynamics of the South American plate: velocities and senses of motion for the different plates and South American tectonic blocks. The study area is among Medellin (M) and La Virginia (V) (Suter, et al. 2008).

The tectonic model of the Jurassic to Cretaceous proposed 2 tectonic settings. The first model suggested that the sedimentary strata and the palaeogeography evolved in an intracontinental rift setting. The second model based on magmatic geochemical data proposed a subduction

extensional setting characterized by the development of a back-arc and intra-arc tectonic setting (Bustamante et al. 2016). During the Late Triassic a breakup of the paleo-Romeral margin developed in an active margin, associated with subduction of the early Farallon plate beginning at ca. 209 Ma (Bustamante et al. 2016; Vinasco, 2019). Over these tectonic episodes, the Cajamarca complex is constrained as Neoproterozoic, but the age of the western part of the Arquía complex is poorly constrained; they may have formed during either the Neoproterozoic or Lower Cretaceous. Between 210 to 115 Ma, the magmatic arc migrated westward, correspondingly to the regional extension after 152 Ma led the opening of the N-S trend marginal seaway (Nivia et al. 2006; Vinasco, 2019).

2.2. Cretaceous to Paleocene

During the Early Cretaceous, the north-western margin of South America experienced the interplay Subduction between the Proto-Caribbean, Farallon Caribbean and Nazca plates (after ca. 25 Ma) (Meschede and Barckhausen 2000; Vinasco, 2019). This interaction involves episodes of extension, subduction, collision and accretion; including the Pangea dissembling, a tholeiitic accretion during the Early to Middle Cretaceous (Vinasco, 2019). This Romeral Fault System has a dextral transpressive kinematic, evidenced in micas recrystallization from Quebradagrande Complex, dated around the Caribbean plate accretion time (Vinasco and Cardoni, 2012).

Initially, the Quebradagrande complex includes a para-autochthonous Late Cretaceous arc remnant, including slices of new formed oceanic crust which have been interpreted as the opening of an ensialic marginal basin (Nivia et al. 2006). Also, an Early Cretaceous sedimentary sequence is known as the Abejorral Fm. (Bürgl and Radelli 1967; Moreno and Pardo 2003; Nivia et al., 2006; Vinasco, 2019). The Cambumbia Stock, a quartz-granodiorite stock, crystalized between ~270 to 112 Ma (Bustamante et al., 2016; Calle et al. 1980; Vinasco, 2018; Spikings et al. 2015). Simultaneously, the Quebradagrande Volcanic member includes an intercalated of quartz-rich sediments with tholeiitic arc characterized by enrichment in LREE and Nb-Ti anomalies that document crustal thickening in an arc system that was already active by ca. 93 Ma (Jaramillo et al. 2017).

2.3. Paleocene to Miocene

Detrital Zircon Fission Track (ZFT) data confirm an Oligocene age for the Lower Member and a Middle Miocene age for the Upper Member of the Amagá Fm. (Piedrahita, et al. 2017). The ZFT age constraining Paleocene to Eocene, late to early Oligocene and late to middle Miocene cooling in sediment source areas mainly located in the Central and Western Cordilleras of Colombia. These ages allow associating the regional exhumation events in the Central Cordillera. The Panama-Choco Block collision against northwestern South America, whereas

the Farallon-Nazca plate subduction, produced a strike-slip reactivation of the Cauca-Romeral fault system, on NW-SE compression tend and NE-SW simple shear trend in the Amagá Basin. This deformational regime, identified by magnetic fabric data, induces syn-depositional and post-depositional deformation over the Amagá Fm. (Piedrahita et al. 2017).

Silvia-Tamayo et al. (2008) constrain the morphology preservation differences between the Amagá Fm. They found that the Lower Amagá had good geomorphology preservation, due to a large and amplitude valley with poor facies variances, while the Upper Amagá had poor preservation, due to continues valley closing and large facies variances. This evidence supported the syn-depositional evolution theory of the Cauca valley and the not well constrain change of kinematic direction, that until upper Miocene continuous as dextral kinematic and during the Choco plate accretion reactivate the Romeral Fault System as sinistral kinematic direction (Peláez, 2016; Ramirez et al. 2012, Vinasco and Cordani, 2012).

2.4. Miocene to Holocene

Mio-Pliocene subaerial volcanic rocks and sub-volcanic intrusions of the Combia Fm. and Combia stock cover and intrude the Amagá Fm. and older rocks (Leal and Mejia, 2019). This is a diorite to granodiorite porphyritic hypabyssal emplacement during Pliocene, which represents the Carnegie Ridge subduction between North-West Ecuador and South-West Colombia. Then the Santa Fe de Antioquia Formation record a tectonic ZFT age which relates this Porphyritic hypabyssal emplacing in 4,8 Ma (Lara et al. 2018).

Additionally, Romeral Fault System evidence a sinistral kinematic and a paleomagnetic rotation of this unit, suggesting a Middle Quaternary change and reactivation in the tectonic at the north part of the Cauca valley (Lara et al. 2018; Piedrahita et al. 2017; Vinasco and Cordani, 2012).

Sandstones from the lower member of the Amagá Fm. display compositional modes, provenance analysis and ZFT ages which suggest sediment sources exclusively associated to the continental South American plate, the proofs from the Early to Middle Miocene Upper Member suggest sediment sources associated to both the South American plate and the allochthonous Panamá-Chocó Block (Lara et al. 2018).

This change in provenance parallels a change in sedimentary environments, from meandering (Lower Member) to braided (Upper Member) rivers, interpreted as a decrease in sediment accommodation space along the northern Andes, this decrease is associated to a regional accelerated uplift in the northern Andes resulting from the Early Miocene accretion of the Panamá - Chocó Block to northern South America (Lara et al. 2018).

3. Methodology and Materials

The field zone located on the northeast of the Cauca-Amagá valley at the Arma and Buey river-mouth limits on the north with Damasco, Antioquia; on the south with Arma, Caldas; the western limit is the Cauca river and the eastern boundary is given by a landscape composed by inclined hillslopes with very limited access (Fig. 1.b). The fieldwork focuses on measure joints, fractures and faults; as well to delimit the morphology changes using the Colombian Geological Survey (SGC) standards. The data process focuses on establishing the paleo-stress tensors and delimit the fluvial, tectonics and denudational geomorphology environment, related to the geologic mapping 1:25000 of the study zone (Fig. 1.b.). The study zone corresponds to the geological maps 166, 167, 186 and 187 scale 1:100.000 by Colombian Geological Survey maps (2009 version); 12,5m DEM (ALOS-POLAR (2011) Satellite in the survey: https://search.asf.alaska.edu/#/, (taken 07/2019)) and 12 field stations (lithology, structural and geomorphology data); which allowed us to control the base map at scale 1:25.000.

3.1. Structural Geology

3.1.1. Joint and fractures analysis:

The joint and fractures study began by establishing the Geology Index Stress (GIS) using the GIS table created by Hoek and Brown (2019), links with the intensity of the joint, the joint connection angles and weathering intensity. For that reason, the table is an approximate base to obtain the trusted value between 90 and 10, where 90 is poorly disintegrated and 10 is too disintegrated. However, we decide to establish the GIS by the heuristic approximation, considering the examples used by Hoek and Brown (2019) which shows different lithology outcrop photos. This represents the main soft spot of the method accuracy because it is not possible to achieve the time to use the complex mathematic formulas.

Hong et al. (2017) associate the GIS with the fractal dimension (FD) (numerical representation of spatial fracture portion), it allows us to compare outcrop stress conditions. The fractal dimension is calculated by the next steps:

- *First, to make 20cm, 80cm and 320cm width photos of the outcrops.*
- *Second, a digital edition of photos with the software Adobe Lightroom to highlight the joint sets, defining white and black photos with quality enhancement.*
- *Third, the photos are georeferenced and scaled in ArcGIS; then each photo is highlight by the joint sets (Fig. 3).*
- *Fourth, establishing the FD value using the Kulatilake et al., (1997) equation, correlating the width of the photo with the joint quantity (Eq 1). Every photo has a GIS and an FD value. Eventually, it is necessary to perform a statistical ponderation of the field data in each field station, analyzing at least 3 different photos per outcrop.*

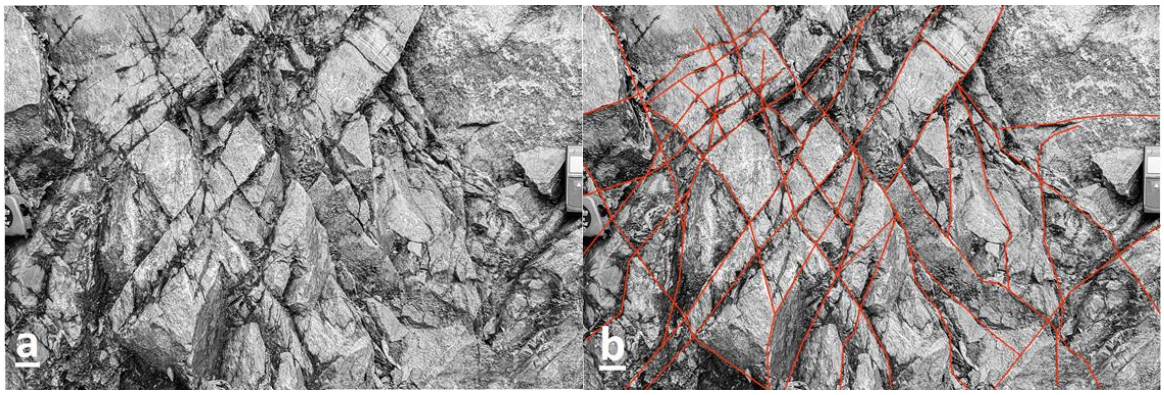

Figure 3. Example of outcrop photographs used for the joint analysis. Field photo corresponds to field station 6.4 (location on Fig 8), 80 cm photo. a. represents the unbounded photo and b. shows the joint and fracture bounded.

The joint sets interpretation uses the dip and dip direction, the FD values, GIS values and the fault distribution; to establish subgroups between lithologies. Besides, the stereo net software helps to visualize the dip and dip direction information (Casas, Gil and Gomez 1990). Furthermore, there is a limitation with the joint field measurements, due to the high physical alteration of the joint plane, especially found in zones with high fragile deformation, resulting in local dip and dip direction changes (Fig. 4). For that reason, some joint dip and dip direction data won't be considered during the analysis process, due to a perturbation produced by the weathering.

Eq.1. Fractal dimension FD equation. Relates the r_i longitude of the photo and $N(r_i)$: Number of joint in the photo.

$$D = \frac{\sum_{i=1}^{N} [\log_{10} N(r_i) \log_{10} r_i]}{\sum_{i=1}^{N} (\log_{10}^2 r_i)}$$

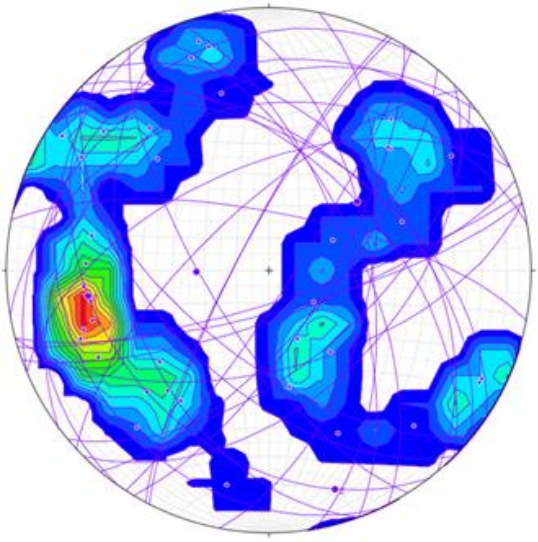

Figure 4. Stereo net illustration the planes on purple and the contours groups, that are represented by the colour zone, illustrate the distribution of the planes poles. For this situation is used the Quebradagrande complex joint data.

3.1.2. Paleo-stress analysis

The paleo-stress analyzes the fault information such as dip, dip direction, fault types, chronology and kinematics evidence (stretch marks, fault displacement, mineral alignment and secondary Riedel fault) (Casas et al. 1990). The paleo-stress implicates a geometrical and stress analysis; based on the main stress axes (s1, s2, s3) and Mohr diagram (Delvaux and Sperner 2003; Žalohar and Vrabec 2008), this base information allows us to process the paleo-stress information using the Win_tensor software (version 5.8.9 of 05/08/2019), to generate the PBT module (P=contraction-axis, B=neutral-axis, T=extension-axis.), Right Dieder method and Stress tensor optimization (Fig. 5) (Delvaux 2012).

- *Initially, the data set is selected into subsets by different stress tensors, lithology configuration and the GIS obtained on the joint analysis, additionally establish the relative timing and reactivation present in the outcrop fault system.*
- *Second, use the Right Dieder method and the PBT axes (Fig. 5 a.&b.), to get the main stress axes and the ratio of principal stress magnitudes (R = (s2 - s3) / (sl - s3)) (Delvaux 2010).*
- *Third, Stress tensor optimization (Fig 5. c.) use the shear stress, normal stress, the dihedral angle and the friction angle (obtained on a Mohr diagram), to improves the accuracy of the tectonic tensor (Delvaux and Sperner 2003).*

The last steps need to be applied repeatedly with the idea of interpreting the complex paleo-stress directions.

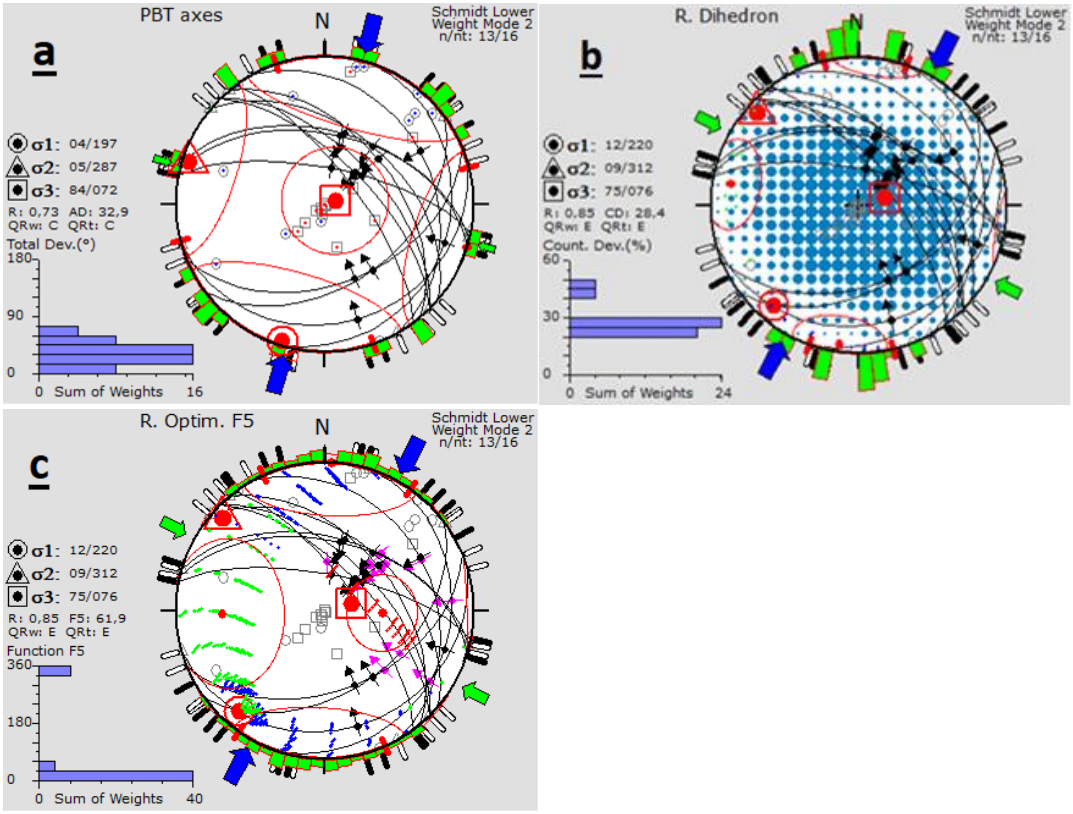

Figure 5. Paleo-stress methods. a. PBT module (P=contraction-axis, B=neutral-axis, T=extension-axis.).

b. Right Dieder method. c. Stress tensor optimization. These stress measurement methods depending on the data quality and the amount of information; but the study zone does not show stretch mark and mineral alignment, due to the weathering and high intense fracture. Also, high weathering condition erases some evidence. To analyze the paleo-stress is necessary to establish the structural facts which control the kinematic development. For this purpose, we considered the statements as follows:

- *Firstly, the micro and macro structures are related by the symmetry principle (Jing et al. 1999; Casas-Sainz et al. 1990).*
- *Secondly, the tectonic respond depends on the rheology of the type rocks, because the igneous, metamorphic and sedimentary rocks react in different ways of stress pulses (Jing et al. 1999).*
- *Third, the tectonic step sequences could create separate tectonic evidence or over-printing tectonic evidence, which means that a NE-SW to NW-SE scenario could create detached evidence or connected evidence by secondary structures.*

3.2. Geomorphology

Morpho-neotectonics research focuses on the relation between landforms and earth surface modification types, brought about by recent tectonic pulses (Panizza and Castaldini, et al., 1987). Examining the impact of tectonism on Holocene landscapes must consider elements that have a little geomorphological inertia, as which tend to erode slowly. Whereas the dynamic nature of rivers and their rapid responses to external changing controls, the sensitivity hierarchy range goes to least to the most sensitive catchment area, interfluves, hillslopes and channels (sensitive) (Burbank and Anderson, 2001). According to the latter, the main drainage basin on the study area is related to the Arma fluvial system, located on a complex structural setting.

3.2.1. Terrain analysis and landform recognition

Before the introduction of the Digital Elevation Models (DEMs), landforms were only identified by the aerial photographs following the methodology in Garbrecht and Martz (2000). Research in geography has used terrain analysis (TA) techniques for topographic analysis and visualization of the land surface features. This includes drainage pattern extraction, river morphology (e.g. Peucker and Douglas, 1975; O'Callaghan and Mark, 1984; Skidmore, 1989; Smith et al., 1990; Band, 1993), watershed delineation (e.g. Jenson and Domingue, 1988; Band, 1986), surface roughness assessment (e.g. Grohmann et al., 2010), monitoring the slope movements (e.g. Wieczorek and Snyder, 2009), predicting the spatial distribution of gully erosion, and soil texture (e.g. Zakerinejad and Maerker, 2014).

Terrain analysis and landform recognition are developed in this order:

- *Available Researches.*
- *Analysis of Geologic and Topographic Maps by the SGC and the Geographic Institute IGAC.*
- *Interpretation of satellite images through Google Earth.*
- *Data processing, using the software ArcGIS. and the topography of the zone obtained from ALOS-POLAR (2011) Satellite in the survey: https://search.asf.alaska.edu/#/, (taken 07/2019); this allowed us to elaborate the DEM, and thematic and schematic maps that finally, integrated with the previous and following analysis, enables to establish the resulting Geomorphologic map.*

3.2.1.1. Planform changes identification: geometry and position:

Channel patterns indicate that they respond to several controls, including sediment size and load, flow velocity, and stream power (Schumm, 1986). Changing channel patterns of the rivers could correlate with differences in their deformation rate, but it is necessary to distinguish between changes in patterns that result from nontectonic and tectonic causes (Burbank and Anderson,

2001). River sinuosity studies (such as those of Adams (1980) in the United States are being useful to identify surface tilting by current and recent tectonics. The conceptual link between sinuosity and tilting involves the analysis of the river slope required to carry the sediment load (Doornkamp, 1986).

The fluvial system is the most sensitive morpho-tectonic environment to changes in gradient and river patterns. Identifying the changes in patterns fluvial planform where deformation may be occurring Sinuosity tends to increase with increased slope (up to a threshold), it might be expected in an active deformation mountain range. It could be revealed by mapping the patterns of the meandering river that shows the sinuosity changes localization along the river course or in a representative temporal change on sinuosity. Similarly, along generally braided rivers, incised zones and single channels bounded by terraces are the candidates for active uplift zones (Burbank and Anderson, 2001)

Planform changes will establish in the results section using a map that shows the fluvial geomorphology of the Arma river system, mapping content is described in the results part

3.2.1.2. River terraces identification:

River terraces are accepted by most workers in the field of neotectonics as an indication that the base level has dropped or that river incision is a response to tectonic uplift or tilting. Before, using the terrace data on morpho-tectonic studies, it is necessary to make certain that the terraces are direct evidence of the neotectonic activity (Doornkamp, 1986).

River terraces can be divided into two classes aggradational and degradational; their configuration in both sides of the river valley and the can be paired or unpaired, relating them using of the cross-section sketches (Burbank and Anderson, 2001). River terraces are detectable using Google Earth's satellite images, the 12,5m DEM and the topographic maps. The previously identified zones of possible river terraces formation can be confirmed during fieldwork and refined with the elaboration of some cross-sections cutting the river channel and the hillslopes beside it; these cross-sections are done using ArcGIS software (Fig. 6).

The aggradational terraces will establish in the results, mapping the Arma river system fluvial geomorphology in the second part of this section: "Geomorphology mapping".

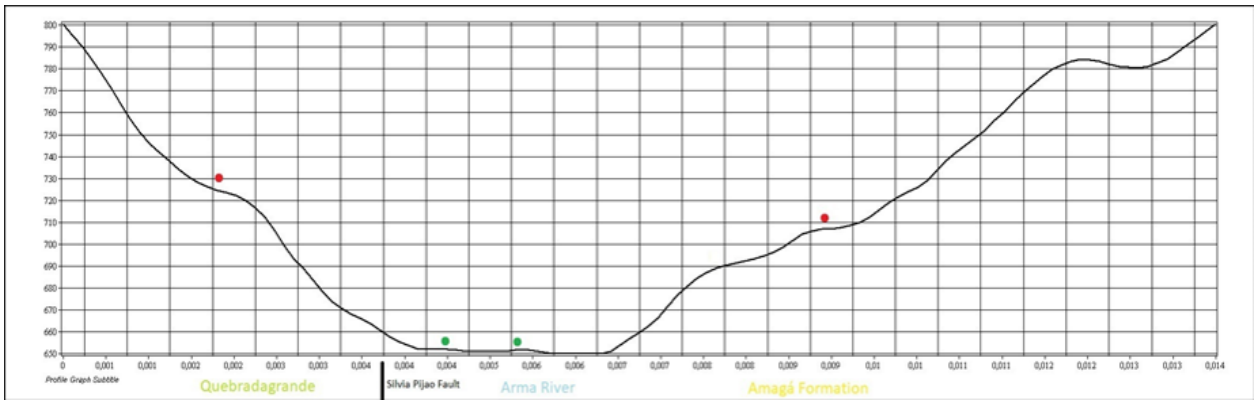

Figure 6. W-E cross-section of the Arma Valley (location of the profile near to the field station 3.2 shown in Figure 14. The green point represents the aggradational terraces and the red points represent the deggradational terraces.

3.2.1.3. Knickpoints identification:

A knickpoint is a topographic area where a stream reach is steepened concerning the adjoining reaches, this situation develops in an absence of tectonism (or eustatic change), due to a difference in the erosion of the bedrock. Tectonically generated knickpoint can be formed through differential folding or faulting of a reach of a river (Burbank and Anderson, 2001).

To understand the dynamic of river systems, John Wesley Powell (1875) introduced the concept of base level: the lower limit of the landscape below which rivers cannot erode. The erosion effect is to cause the knick-point to migrate or propagate upstream. As the knickpoint migrates through, the reach is steepened, stream power increases, more sediment is eroded than is deposited, and the bed is lowered until it is approximately graded to the adjacent downstream reach. The multiple events of incision and aggradation represent a complex response to simple base-level lowering (Burbank and Anderson, 2001)

Knickpoints are determined through the analysis of topographic maps, but also geologic maps, to determine where knickpoint are a response to structural or lithological context (Fig. 16.). A more refined analysis of the terrain is made using ArcGIS and DEM's to determine visible slope changes. Previous identified points with a longitudinal section along the river course, configured used the interpolate Shape gadget to add the elevation information, through Z min (interpolate the minimum z data around the line), Z lineal (interpolate just the z data along the line) and Z closest (interpolate the closest z data around the line).

3.2.2. Geomorphology mapping

Geomorphic mapping at small scales is dominated by structural forms, at larger scales or more detailed, where the main forms are due to climatic processes (Gutierrez, 2008). The scale of work established in the current work is regional to semi-detailed, 1:25.000 m, covering an area of about 206 km2. The minimum area that can be mapped is 25.600 km2, for the topographic data obtained from ALOS-POLAR (2011) satellite in https://search.asf.alaska.edu/#/

There are many legends for geomorphologic maps to classify the different morphologies and also differential needs and priorities according to each country or region. Geomorphology mapping for this study is based on the guide: "Guía Metodológica para la Zonificación de Amenaza por Movimientos en Masa Escala 1:25000" (SGC, 2017). We used geographic units in the MAGNA SIRGASS Coordinate System, with Bogotá as its origin.

3.2.2.1. Geomorphological map:

Geomorphological maps for this study are made according to the next criteria:

- *Geomorphic environments:*

The most evident processes that are affecting the landscape correspond with three geomorphic environments: tectonic, fluvial and denudational (Fig. 7. a.&.b.). The geoforms associated with these, are summarized in Chapter 3 of the SGC (2017) guide where the symbology and classification are simplified (Table. 1).

- *Hillslopes:*

Hillslopes can be constituted by rock mass or soils; they show different mechanic properties and evolution (Gutierrez, 2008). Hillslopes mapping is described in three ways (Young, 1972): morphologic maps, slope´s maps and genetic geomorphologic maps. The last one is the most used in geomorphic mapping; it relates geoforms to their possible origin (Gutierrez, 2008). We follow the criteria for hillslope identification proposed in SGC (2017)

- *Unconsolidated deposits and landslides:*

It seems evident that relief energy, geometry (height, longitude and form) and exposure of hillslope constitute the prior landslide causes. The hillslope geometry modification is common and mostly respond to fluvial or littoral erosion (undercut river bank), dissolution, artificial causes, among others (Brunsden, 1979; Borgatti and Soldati, 2005).

A landslide is the movement of the rock mass, debris or earth downside a hillslope. This study follows Varnes (1978), who created the landslides classification, it classifies according to the affected rocks character and movement type, but there are so many other classifications, e.g. Skempton and Hutchinson (1969), Hutchinson (1988), Epoch (1993), (Gutierrez, 2008).

For landslides and deposits recognition through, the methodology is based on the use of satellite images to detect major landslides, and some in the fieldwork to confirmed through a detailed analysis of aerial photographs and DEM.

Tectonic Environment		
Morphology name	***R,G,B***	***Abbreviation***
Structural triangular facet	200,200,250	STF
Structural triangular facet-bearing	247,178,246	STFb
Structural Ridge	227,205,247	SR
Structural Shutter Ridges	222,200,238	SSR
Structural Staggered slopes	240,163,207	SSs
Structural denudation hill	255,205,243	SDh
Denudational Environment		
Residual Hill	240,170,40	DRh
Superior erosion scarp	150,120,25	DSEs
Minor erosion scarp	165,130,85	DMEs
Erosive hillside	204,195,100	DEh
Undulate hillside	247,244,136	DUh
Denuded hill	160,140,110	DDh
Denuded loin	227,175,107	DD
Fluvial Environment		
Longitudinal bar	71,95,135	FLb
Central Barr	191,215,255	FCb
Ejection cone	215,245,255	FEc
Accumulation Terrace	160,210,255	FAt

Table 1. Summarizes the morphology elements and the colour index

3.2.2.2. Arma River Fluvial System map:

To provide higher resolution geomorphological analysis, we elaborate a detailed map of the Arma river Fluvial System, along with other geomorphologies represented in the Geomorphological Map (Fig. 17).

This map (Fig. 18) represents the geometry of aggradational terraces, barrier deposits and the river system pattern over the channel course in the study zone. Enables the identification of zones where the river channel changes to be more sinuous or braided. It also allows us to analyze the river terraces continuity along the river trace.

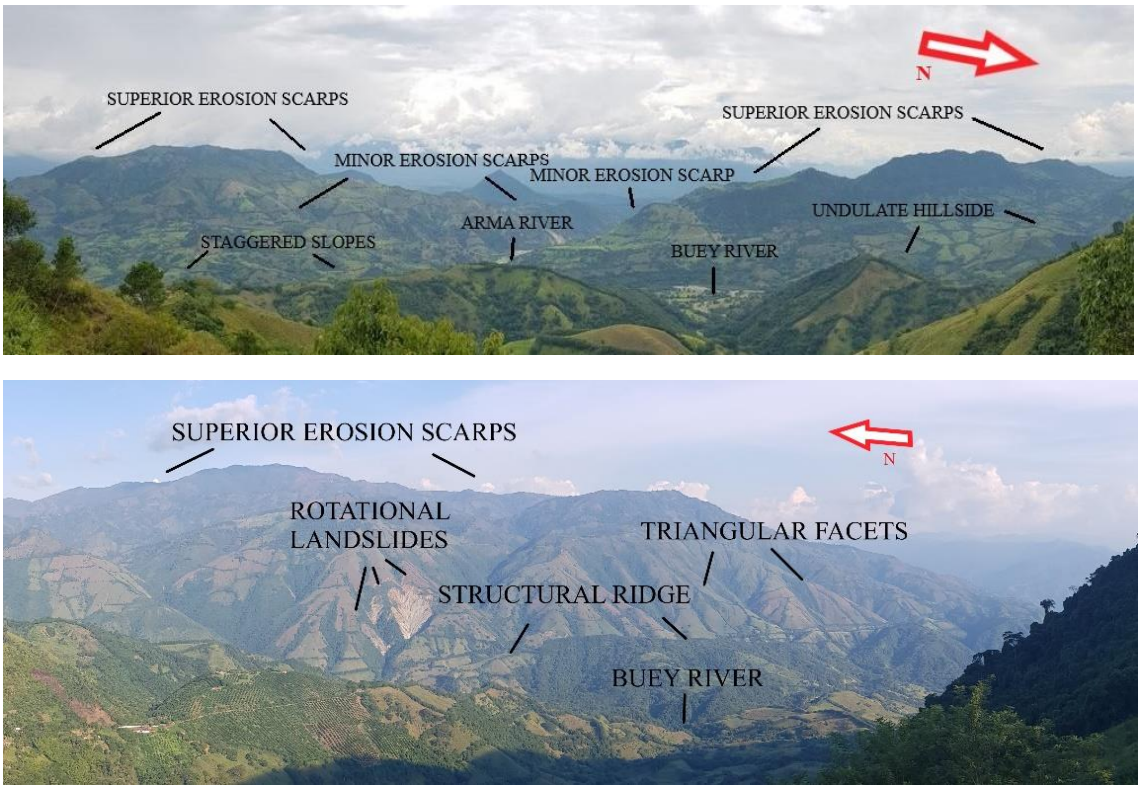

Figure 7. Landscaped photos with the geomorphology description. a. Represents the west part of the study zone. b. Shows the northeast part of the foothill.

4. Results

4.1. Mapping results

We produced a geological map 1:25000 shown in figure (Fig. 8). We refined several misfits due to fault trace over the east part of the Silvia-Pijao fault, while on the west part of this fault the accommodation of the Amagá Fm and the Combia Fm and Combia stock is controlled by the morphology (Fig. 8.).

The Cajamarca and Quebradagrande complexes are limited by the Arma fault, evidenced as a fragile-ductile deformation with fault propagation folds, also on the east side limited to Cajamarca complex shows a clay band (Fig. 9.a. station 3.3).

Figure 9. Outcrop structures. a. Station 3.1 shows the fault limit between Cajamarca and Quebradagrande complex. b. Station 5.1 evidence a positive flower structure (evidenced by Riddle fault kinematic).

Intense deformation and high weathering masks the W-E contact between the Cajamarca complex and the Santa Barbara Metagabbro. Typical transpressive structures are documented in the field, such as positive flower structure (Fig. 9.b. station 5.3.) in the Combia Stock (evidenced by Riddle fault kinematic). The Quebradagrande complex is found over the south-east (Fig. 8. station 6.1) where previously mapped as the Amagá Fm., also the Quebradagrande complex is controlled by the Piedecusta and Silvia-Pijao faults. Furthermore, the Silvia-Pijao fault trace considers the geomorphology evidence in structural ridges, triangular facets and river alignment and the station 5.1 evidences; helps to delimitate the fault behaviour and extension.

Next Page: Figure 8. Geologic map 1:25.000. This map shows updated boundaries and fault traces such as the Silvia-Pijao Fault on the south part of the Arma Fault, the Quebradagrande complex around the station 6.1 and the Cajamarca complex on the east side of the Silvia-Pijao fault.

Geologic Map

Escobar, S., Mesa, S.

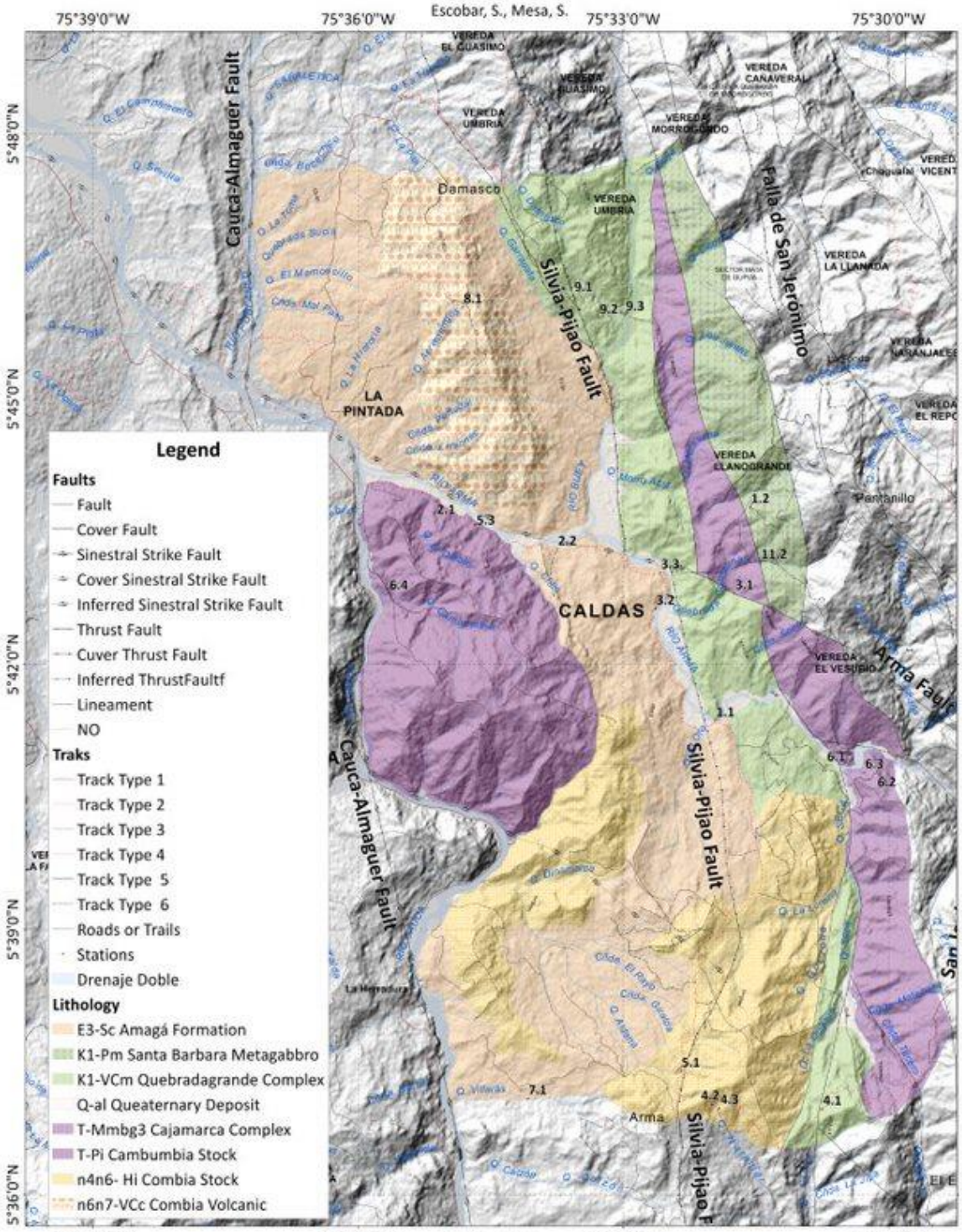

4.2. Structural analysis

We consider dividing the area into five structural blocks delimited by the main fault structures as shown in Figure 10. Block 1) between Arma, San Jeronimo, Silvia-Pijao and Piedemonte faults. This block is composed by the Cajamarca and Quebradagrande complex. Block 2) between Cauca-Almaguer, Silvia-Pijao and unnamed fault; this structural block represents the middle part of the field zone, it has Cambumbia Stock, Amagá Fm. and Combia Stock member. Block 3) between Silvia-Pijao, Arma and an unnamed fault on the East of the Silvia-Pijao fault, it contains the Quebradagrande complex and Combia intrusive member. Block 4) between the unnamed fault on the East of the Silvia-Pijao, Arma and San Jeronimo fault, this block is composed by the Quebradagrande Complex. Block 5) between Cauca-Almaguer, Silvia-Pijao and an unnamed fault, this block represents the southwestern zone, it contains Combia Stock member and Amagá Fm. These structural blocks and lithologies are the configuration settings for constrain and analysis of results

4.2.1. Joint and fracture analysis

The GIS shows a trusted range between 20 to 67.5 (Fig. 11); this is divided into two groups: 20 to 43.3 and 60 to 67.5; the first group correspond to a middle to advance weathering and angularity to disintegrated blocky condition. The second group correspond to quarry and road outcrop that is preserved in a good weathering condition and preservation of the angularity blocky condition (Fig. 11). The FD shows a value range between 0.62 to 0.92 (Fig. 11), this range is divided into 3 groups 0.62 to 0.73, 0.76 to 0.83 and 0.9 to 0.92 (Table. 2); this increase of density represents the scenarios of 1 to 3 joint sets and secondary fracture proceed by advance weathering.

In another hand, The GIS and the FD help to determinate the possibility of joint displacement, it produces an irregularity among the direction on the sets, this is due to the advance to middle weathering that generate instability by almost 90° fractures, additionally, The Cauca-Almaguer-Silvia-Pijao fault system produces constant seismic episodes that encourage the displacement on the joints. For this reason, the Table. 3 remove the ~90° non-tectonic joints data and average the dip and dip direction of the joint sets over every station.

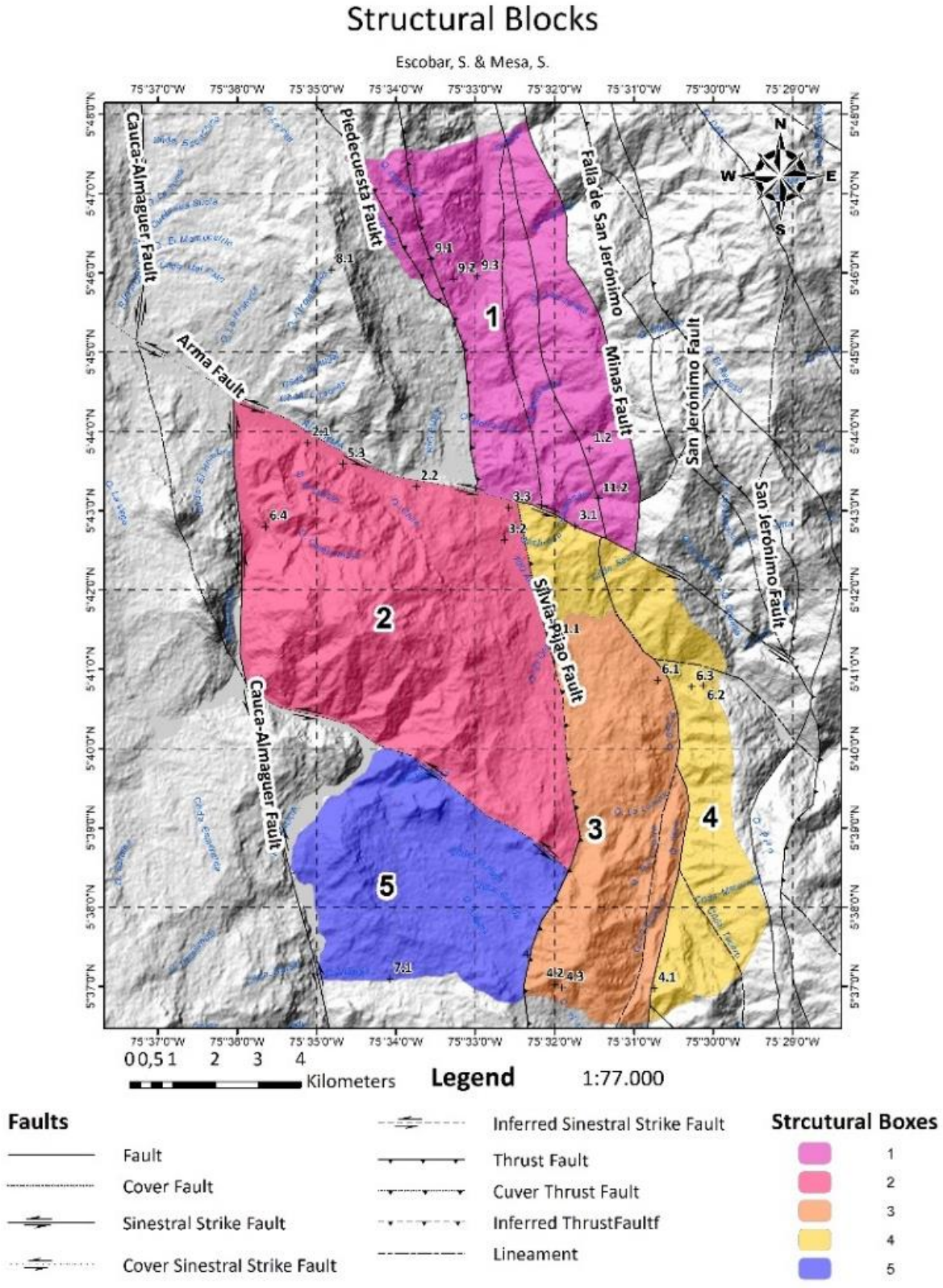

Figure 10. Structural blocks map. This map illustrates the limits of the structural block configuration.

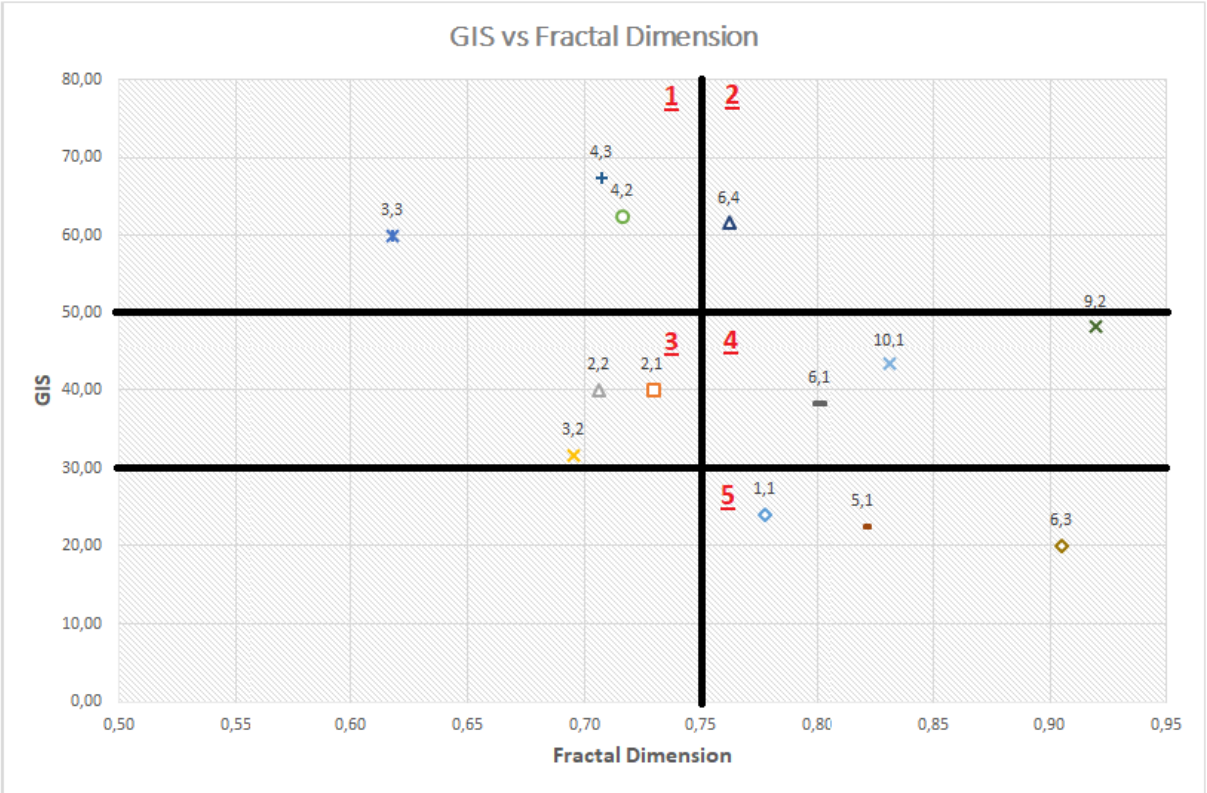

Figure 11. GIS vs FD chart grouped the evidence in 5 Fields. Fields 1 and 2 represent a well preserve blocky outcrop, related to the anthropic intervention. Field 3 shows less fragile deformation with middle weathering process. Fields 4 and 5 both are controlled by the Romeral Fault System; however, the increase of weathering depends on the distance of the faults.

Block #1 presents a joint set between the Cajamarca complex, Santa Barbara Metagabbro and The Quebradagrande complex split into three joint sets providing only NE-SW and NW-SE trends. Block #2 presents the Cambumbia Stock with three tectonic trends NE-SW, NW-SE and W-E trend; in general, split into 3 joint sets. Whereas the Amagá Fm. shows 2 and 3 joint sets with an over-print rotation NE-SW to NW-SE. Block #3 has multiple fractures over the Quebradagrande complex shows 2 joint sets with NW-SE tectonic trend, while the Combia Stock illustrate NE-SW and NW-SE trend between 3 joint sets (Fig. 12). Block #4 presents the Cajamarca complex with NW-SE tectonics trend and The Quebradagrande complex with N-S tectonic trend (Fig. 12.d.). Block #5 shows an over-print event among W-E, NW-SE and N-S tectonic trends over the Combia Stock and the Amagá Fm.

ID	Data Type	20cm	80cm	320cm	Average
1,1	GIS	35	20	40	24,03
	F. Dimention	1,03181532	0,69477497	0,6061569	0,78
2,1	GIS	45	40	35	40,00
	F. Dimention	0,85620113	0,71553518	0,61635753	0,73
2,2	GIS	35	40	45	40,00
	F. Dimention	0,85620113	0,61799036	0,64378735	0,71
3,2	GIS	30	30	35	31,67
	F. Dimention	0,73345158	0,6465532	0,70688463	0,70
3,3	GIS	70	60	50	60,00
	F. Dimention	0,64956077	0,63271836	0,57136849	0,62
4,2	GIS	65	60		62,50
	F. Dimention	0,64956077	0,78365275		0,72
4,3	GIS	65	70		67,50
	F. Dimention	0,76862179	0,6465532		0,71
5,1	GIS	25	20		22,50
	F. Dimention	0,94574985	0,69477497		0,82
6,1	GIS	35	40	40	38,33
	F. Dimention	1,06086043	0,78365275	0,55802647	0,80
6,3	GIS	25	15	20	20,00
	F. Dimention	1,08757934	0,88813251	0,73898104	0,90
6,4	GIS	65	60	60	61,67
	F. Dimention	0,53724357	0,96952748	0,78009003	0,76
9,2	GIS	55	45	45	48,33
	F. Dimention	1,26319353	0,93051407	0,5648258	0,92
10,1	GIS	40	40	50	43,33
	F. Dimention	1,08757934	0,72524749	0,68162393	0,83

Table. 2. Summary of GIS and FD value per station. The chart relates GIS vs FD and shows the different groups.

Date	Station	Set #	Avarage Dip	Avarage Dip direct	N°	#Bloque	Trend
2	1	J1	56,29	48,86	7	2	NE-SW NW-SE
		J2	66,00	137,44	9		
		J3	49,43	235,14	7		
2	2	J1	69,00	41,33	3	2	NE-SW NW-SE
		J2	42,50	299,00	2		
		J3	78,50	102,50	2		
3	1	J1	57,67	48,33	3	4	N-S
		J2	62,60	164,20	5		
3	2	J1	55,20	218,20	5	2	NE-SW NW-SE
		J2	50,00	31,67	3		
		J3	78,50	153,00	2		
3	3	J1	65,75	139,75	4	2	N-S NW-SE
		J2	45,00	303,00	4		
		J3	73,00	60,50	4		
4	2	J1	62,60	84,80	5	3	W-E
4	3	J1	65,00	50,67	3	3	N-S NW-SE
		J2	61,50	231,25	4		
		J3	70,80	313,00	5		
5	1	J1	71,50	173,75	4	5	N-S W-E
		J2	61,00	279,50	2		
5	3	J1	61,00	76,20	5	2	W-E
6	1	J1	62,17	132,39	23	3	NW-SE
		J2	75,00	292,50	2		
6	3	J1	59,50	114,00	2	4	NW-SE
		J2	76,00	312,00	1		
6	4	J1	75,50	320,75	4	2	NW-SE
		J2	64,00	212,20	5		
		J3	26,60	331,00	5		
7	1	J1	60,91	158,82	11	5	NW-SE W-E
		J2	27,83	259,60	5		
		J3	41,33	143,33	3		
9	2	J1	66,50	57,67	6	1	NE-SW NW-SE
		J2	80,00	289,00	1		
		J3	58,00	336,00	1		
10	1	J1	42,50	269,17	3	2	NE-SW NW-Se
		J2	38,50	345,50	2		
11	2	J1	45,00	244,00	5	1	NE-SW

Table. 3. Joint table analysis. Summarizes the dip and Dip direction per field station by averaging each joint set. Additionally, figure 12 represents a plane and stereonet the families and joint preference direction.

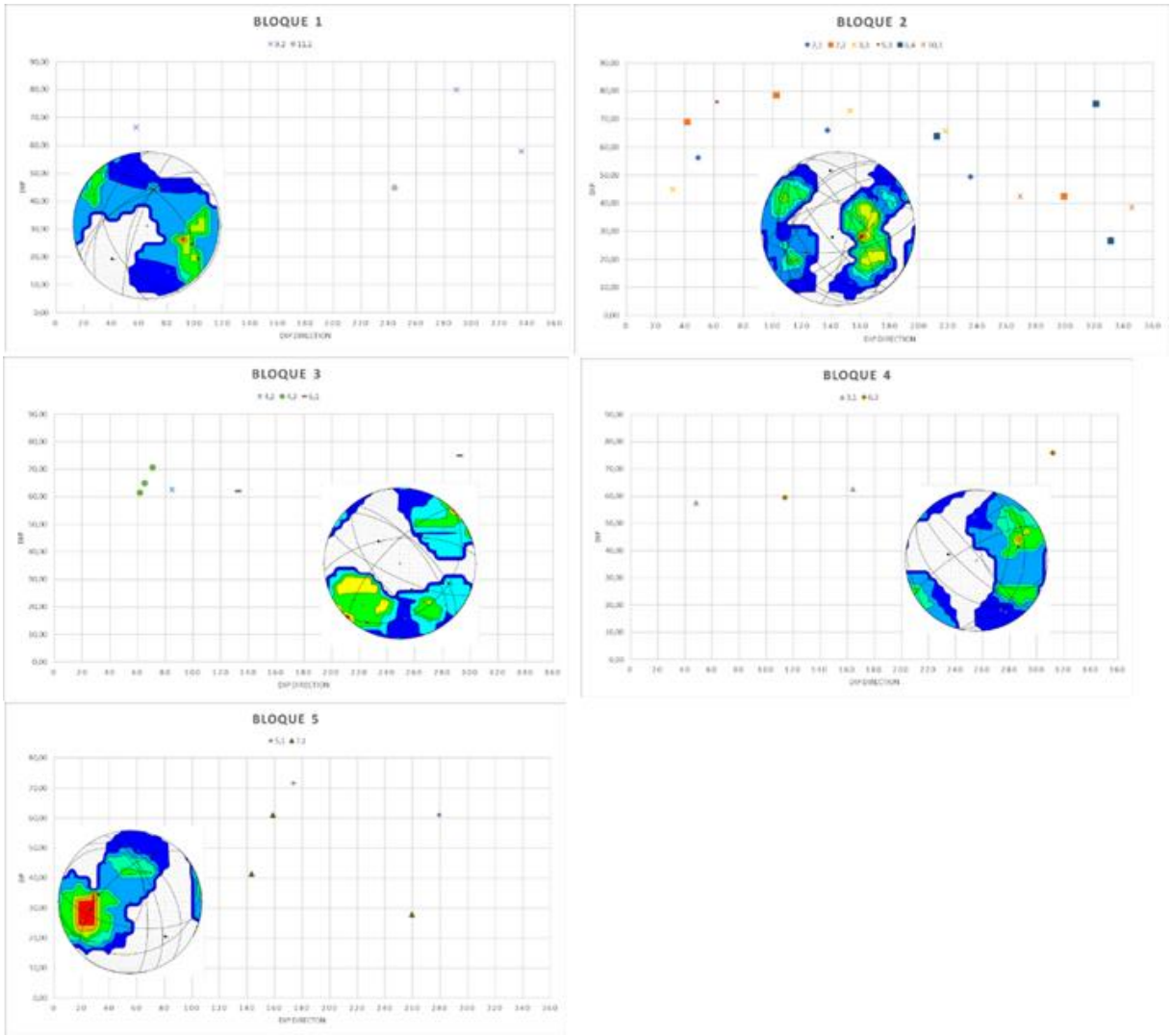

Figure 12. Joint and stereo net charts. These relate the data from table 3. Graphing the azimuth vs dip and the stereo net visualization in the 5 structural blocks.

4.2.2. Paleo-stress analysis

The Paleo-stress analyses 104 fault dip, dip direction and fault kinematics, showing that the fault displacement and secondary Riedel faults are the most of the evidence with the 70%, the Augen, fault displacement, stretch marks and mineral alignments with the 30%. The structural block segments show a variable condition, the blocks #1 and #4 correspond to Quebradagrande and Cajamarca Complex, exhibit a stress direction change from NE-SW dextral-reverse to NW-SE dextral (Fig. 13. Stations 6.1, 9.2 and 11.2). The block #2 exhibits two different behaviours, NE-SW sinestral-normal present in Cambumbia Stock and NW-SE sinestral-reverse present in the Amagá Fm. The block #3 express an NW-SE sinestral-reverse kinematic over Combia Stock, also a NE-SW normal kinematic over Quebradagrande Complex. Block #5 has a smaller number of faults but shows a NE-SW reverse kinematic over the Combia Stock and the Amagá

Formation. As a summary, there are 3 different tectonic stress set NE-SW dextral-reverse, NW-SE sinestral-reverse and N-S sinestral-reverse (Fig. 13).

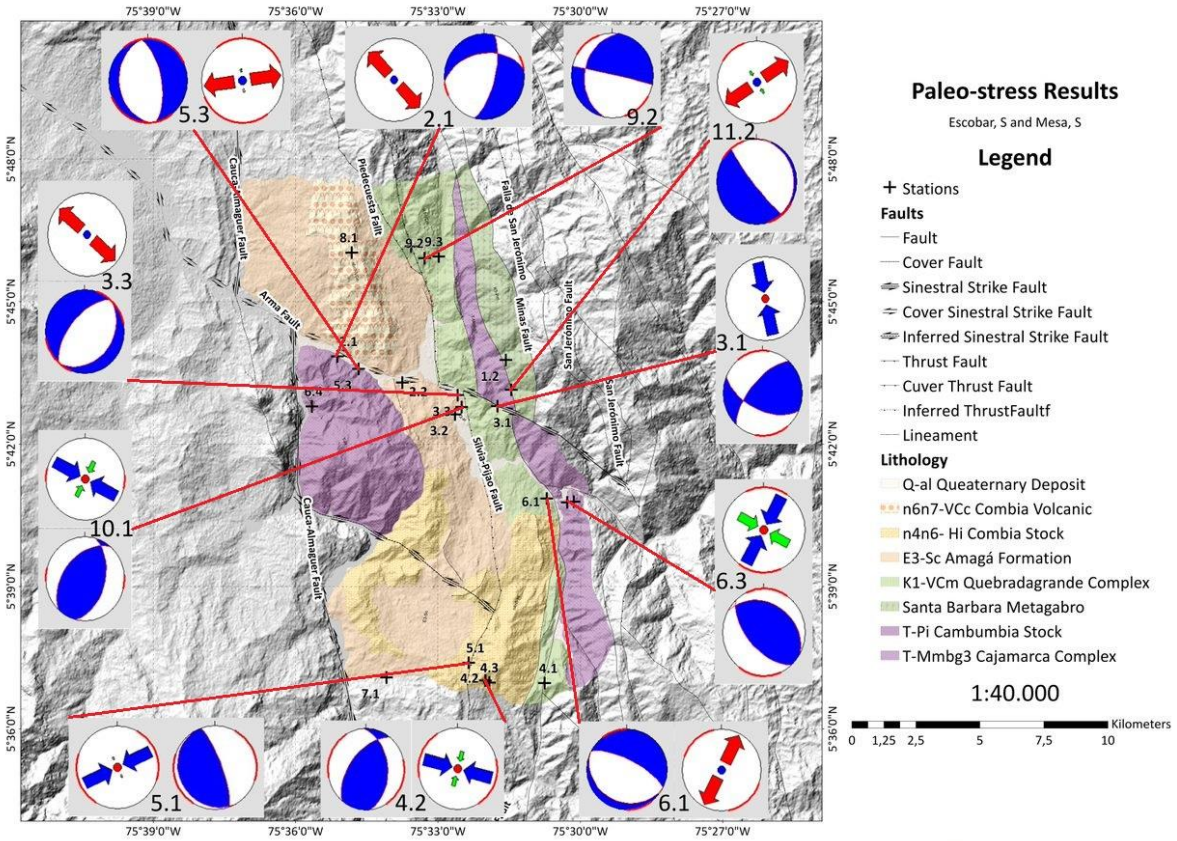

Figure 13. Paleo-stress map. It organizes the focal mechanism and the main stress tensor per station Geomorphology Results.

4.3.1. River terraces identification

The aggradational and degradational terraces were interpreted using cross-sections Arma river, Buey river, Seca creek and Grande creek; these are the main river valleys in the field zone. The cross-sections and the Hillshade layer are the base information to interpret hillslope behaviour. It is worth to say, that the cross-section along the Arma river, Buey river and Secas creek (Fig. 14) shows 3 events of deposition over the ejection cones.

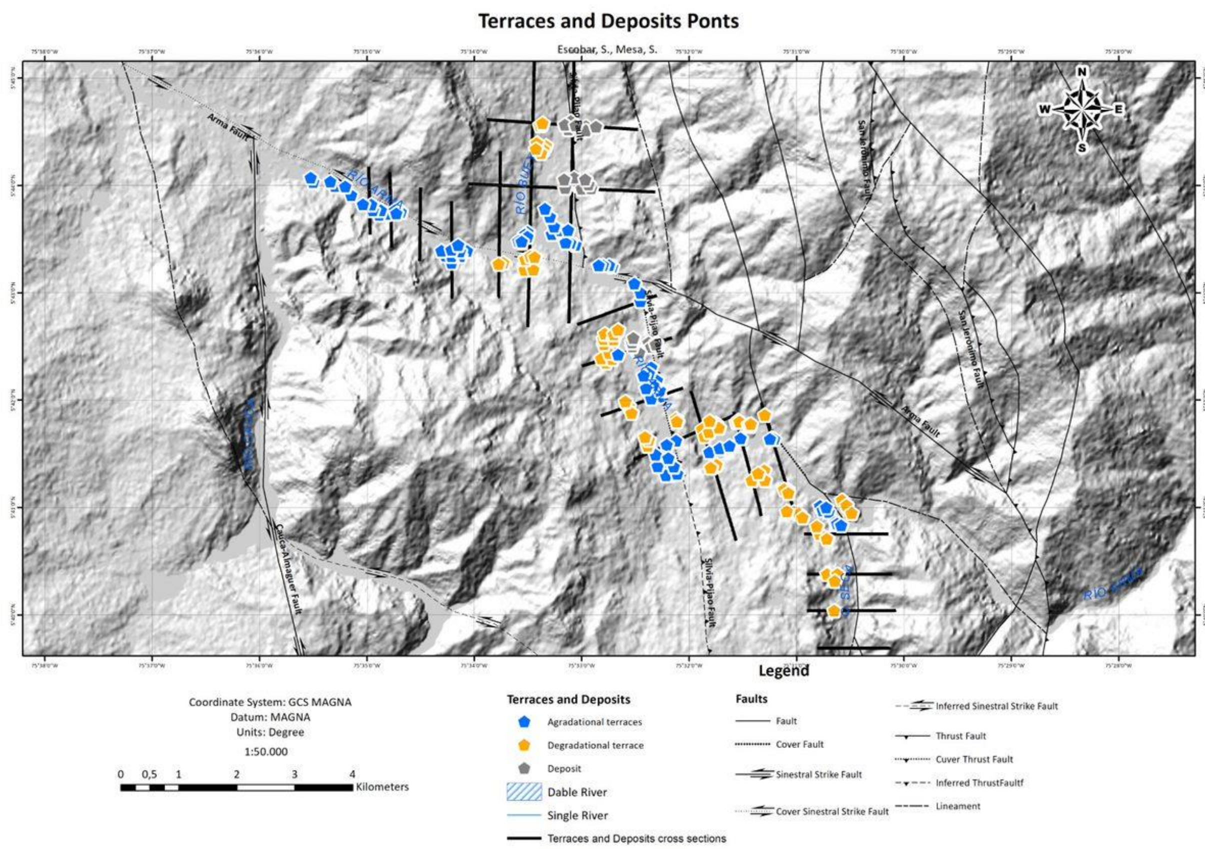

Figure 14. Terraces and deposits point map. This map shows the degradational, aggradational and colluvial deposits as a represented in a layer of points, which is the information base (coordinates and height) for the Fig. 15.

To relate the height of the aggradational, degradational and ejection cones are established as a point layer, to interpolate the coordinates and the elevation data, then plotted into an X-Y chart; combining the north coordinates with the height (Fig. 15a), and the west coordinates with the height (Fig. 15b).

The longitude vs the height chart (Fig. 15.a) shows a decreasing behaviour for the aggradational and degradational terraces, but the ejection cons show a comparable elevation, except the northwards deposits which are over 20m over them (Fig. 15.a). The degradational terraces show a high-height above sea level irregularity with a range between 876.86m to 643.086m just over 600m downstream. The aggradational terrace has a low angle decrease with an elevation range between 700m to 610m, these terraces are subdividing according to the channel patterns.

The latitude vs the height diagram (Fig. 15.b) shows 2 groups of degradational terraces establish by the hillslope change around 700m height above sea level because the degradational terraces belong this height above sea level has a low angle slope and are closer to the aggredational

terrace and colluvial deposits. While the degradational terraces above the 700m correspond to the south-eastern and higher part of the Arma river, showing more spacings between terraces.

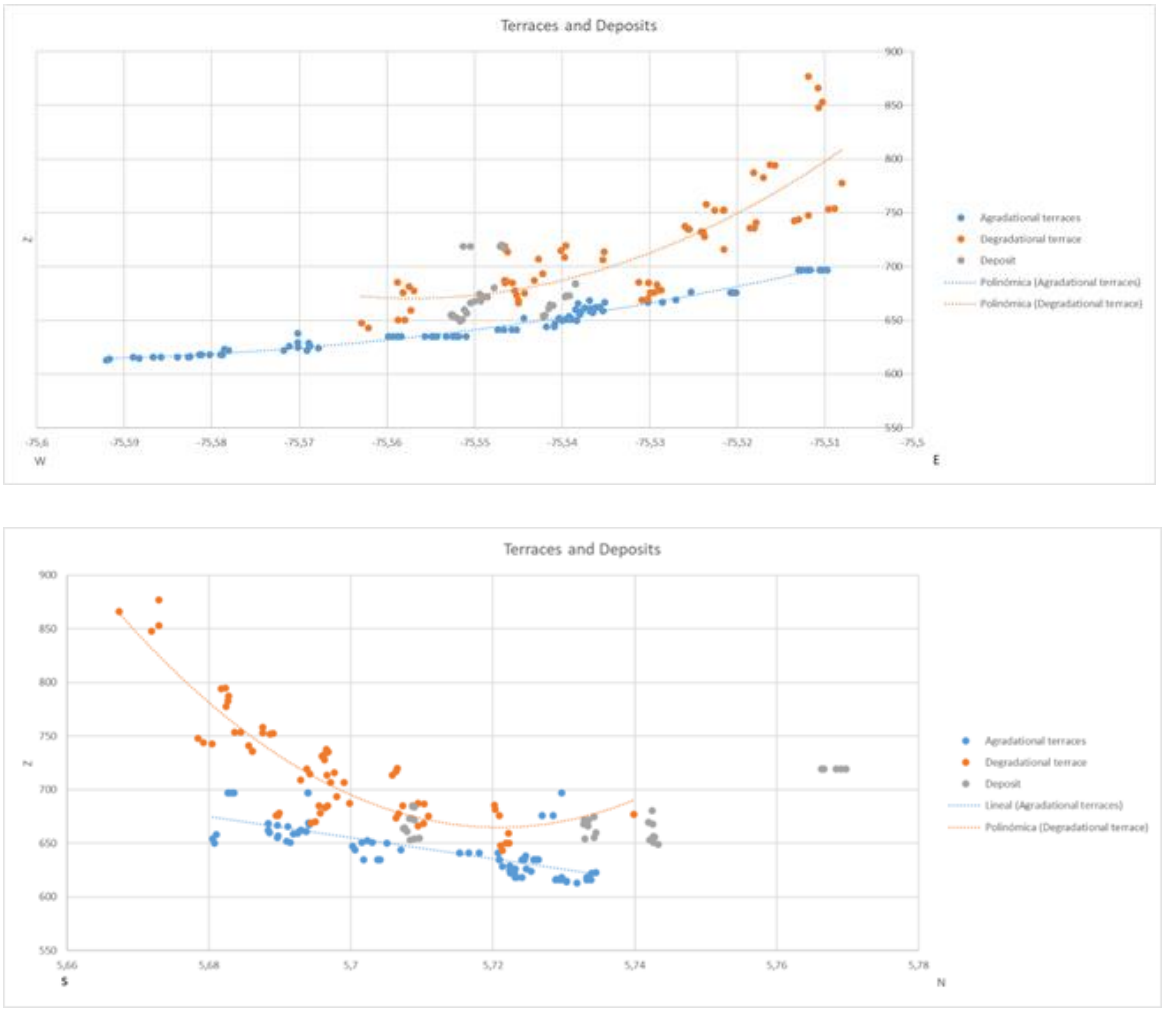

Figure 15. Coordinates (axe X) vs Height (axe Y) of terraces and colluvial deposits. a. This chart relates the longitudinal position and elevation. b. This chart relates the latitude position and height.

4.3.2. Knickpoints identification

We present in Figure 16 the results of the knickpoint analysis. This longitudinal section goes from upstream SE to NW Arma river mouth; at 2km it's shown the first knickpoint, produced by an unnamed fault among the San Jeronimo and Silvia-Pijao fault system, this section is surrounded by a lithological change of the Cajamarca complex to the Quebradagrande complex on the left side and the right side preserves the Cajamarca (downstream). At 3.5km the end of the river alignment by an unnamed NW-SE fault changes the river direction and produces a

knickpoint, lithology changes over the left side, from the Cajamarca complex to the Quebradagrande complex leaving this section, the river is surrounded only for the Cretaceous Complex.

At 4.7 km the Silvia-Pijao fault started alignment of a river section and the left side lithology change between Quebradagrande complex and Amagá Fm. produce the next knickpoint. However, at 7.9km the river leaves the Silvia-Pijao´s control and that produces another knickpoint. Downstream at 9.4km the Arma fault generates a knickpoint and aligned the river until the river mouth. The last stretch of the Arma river is among 11.2km and 15km, where at 12.4km a knickpoint is produced between the Amagá Fm. and the Combia Fm. (on the left downstream), at 12.4km and 13.9km the Amagá Fm. knickpoint to Combia Fm.

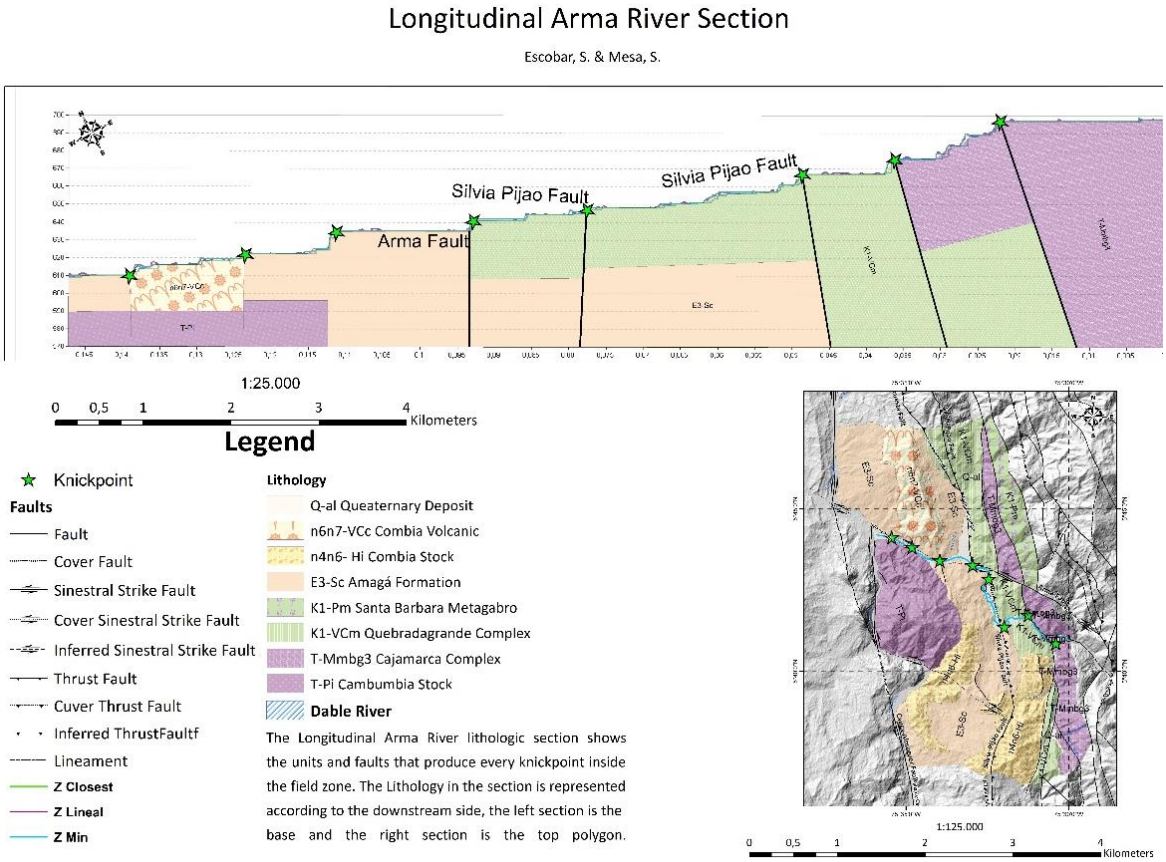

Figure 16. Longitudinal geological section along the Arma river. This section links the altitudinal changes along the Arma river with the lithology configuration of the valley. The lithology in the section is represented according to de downstream side, the left section is the base and the right section is the top of the scheme.

4.3.3. Geomorphological map

This map is the result of terrain analysis detection and landform recognition, fieldwork, description and delimitation of geomorphologic expressions and landforms within a scale of 1:25000 for the established investigation area (Fig.17). The main geomorphic environments identified in the area are structural, denudational and fluvial, but other important processes are occurring as, landslides and anthropic land use and modification.

Geomorphologic expressions of tectonic processes are evident in the zone, the resulting forms tend in general to be controlled by the orientation of Cauca-Almaguer and Silvia-Pijao fault Systems. An important amount of structural tectonic morphologies occurs beside Silvia-Pijao's, taking it as a reference point to understand the geomorphologic processes associated.

The west side of Silvia-Pijao is a zone where the main responses of the terrain to tectonic deformation are structural staggering slopes, in general, they have medium longitudes and moderate slopes with staggering geometry. They are represented along the center area of the map occupying it from north to south, principally over rocks of the Amagá Fm.; other tectonic geomorphologic landforms in this area are two Structural denudation hills that can be detectable, they follow the main N-S orientation; additionally, on the outermost western area, there are at least 5 triangular facets formed as a reaction to the presence of one inferred strike fault with NW-SE direction, between Cauca-Almaguer and Arma faults, this interaction also affects the Cauca river direction. Furthermore, this fault interaction form two Structural ridges where Arma fault displaces the Silvia-Pijao fault System; another two structural ridges are formed close, beneath Seca creek, but they follow a more N-S direction, then, they correspond to the other side of Silvia-Pijao fault, a reference point.

In the study zone on the east of Silvia-Pijao fault, the tectonic landforms represent the lowest zone of the western foothill landscape, thus, the presence of structural triangular facets is abundant, highlighting two shorter triangular facets close to two structural ridges along with the Seca creek. Moreover, the bigger and numerous facets occur especially in the northern sector at Buey river Basin, where two levels of facets are distinguishable suggesting two uplift events that generated them, the lower ones are the shorter facets; in this area another structural ridge can be observed, following the trend of Silvia-Pijao fault, positioned over one unnamed fault of the system, on the west of this geomorphologic structure there is a Structural denudation hill, as it is evident the structural control on its orientation but with elevated weathering processes on it. As Buey river gets to its river mouth in Arma river, facets tend to be more rounded, and, given the presence of another structure: Arma fault, more weathering can occur, modelling two Structural triangular facets-bearing, at both sides of Campanas creek, above one triangular facet.

Denudational processes are affecting the whole zone; Superior erosion scarps, are forming in the presence of crystalline rocks and in general at the highest elevations, Volcanic rocks of Combia Fm. and the Combia Stock, in the northern and southern area respectively, are exposed within abrupt slopes, long hillslopes and in general a concave geometry, Cambumbia Stock has long and high steepened hillslopes with a more irregular geometry but in general concave, the other Superior erosion scarps are forming in the northeastern zone in the rocks of Santa Barbara Metaggabro at the base of the foothill.

The minor erosion scarps tend to appear beneath superiors; in the southeast, they affect Cajamarca Complex; along the southwest margin, appear over Combia Stock, and in the middle to lower elevations of Cambumbia Stock in the Central Zone. Minor erosion scarps appear in the northern area associated with the lower parts of the Combia Stock, but these scarps tend to be shorter and less representative than the others.

At lower elevations and in general, affecting Amagá Formation, appear some erosive hillsides, they tend to have short extensions, slopes that are moderate and in general, with irregular or concave geometries; moreover, Amagá Fm. in the north and south sections of the map, has a presence of undulate hillsides and denuded loins, both with moderate slopes and medium to short extensions. In the zone, one Denuded hill, on the southwestern area, positioned at the south of two structural ridges, this hill can be related with the Structural denudation hills that continue with this tendency in the north, but weathering agents affect this one more, to determine it as a tectonic resulting form (Fig. 17).

Landslides in the study zone detected on the east of Silvia-Pijao fault, affecting the Superior's and Minor's erosion scarps, but there is a case where a short Translational landslide is in the eastern slope of one of the two large Structural ridges in the southeast section of the whole area. In the Buey river Basin, at the north, one large Rotational landslide and two shorter are affecting the upper part of two Structural triangular facets, additionally, these landslides are positioned above an unnamed fault of the system; advancing to the south; between a group of triangular facets and two triangular facets-bearing there is a group of medium to short landslides; three Translational landslides and one creep in the northern Superior scarp and two rotational and one Translational landslide in the Superior scarp of the south, otherwise, in the Superior erosion scarp above the two triangular facets-bearing, two medium to large rotational landslides are present, they are also over the same unnamed fault mentioned previously, that has some role defining the two levels of facets, and is the same fault that controls the structural ridges in the south area. In the southeast outermost zone, there is a group of resulting forms affecting the Minor erosion scarp of Cajamarca complex, 3 medium Rotational landslides, two short Translational landslides and one Creep process; Minor erosion scarps of Quebradagrande complex with the presence of 4 Translational landslides, one of them are larger, than the others shorter (Fig. 17).

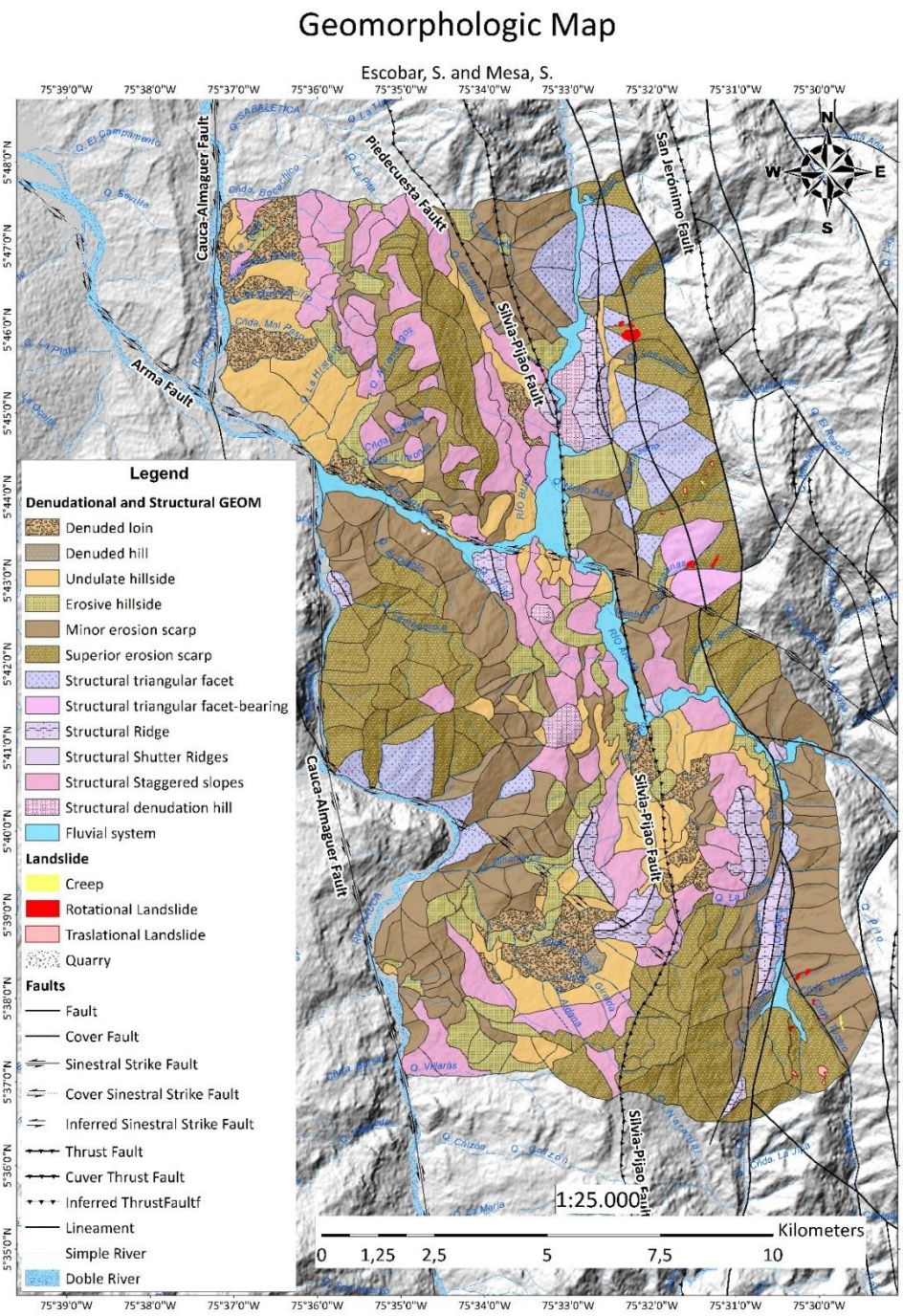

Figure 17. Geomorphologic map 1:25.000. Represents the denudational and tectonic environments and the landslides are including.

Fluvial system study is focused on Arma river, presented with a map (Fig. 18.) as another result in this section, nonetheless; fluvial system in the zone in general, at least the bigger river formations, seems to be directly controlled by the presence of faulting structures, the bigger rivers and basins present are Arma river basin and Buey river basin, tributaries have in general dendritic drainage patterns, except along the western foothills, where drainage tend to be straight, similarly, happens at the western side of Combia Volcanic rocks, but drainage have to advance through rocks of the Amagá formation, then straight patterns here are more irregular. Some tributaries charge big amounts of material that are being deposited during short periods, in ejection cones form, analyzed in the Arma Fluvial System Map result section.

The human interactions within the terrain are important to consider; in the zone, anthropogenic modifications of the landscape are due to multiple activities and uses; in the geologic map, roads, tracks and trails and urban settlements are represented, the geomorphologic map shows the presence of two small quarries, one of them is localized near stations 2.1 and 5.3 between the main road and Arma river, they extract fluvial sediment material from it; the other quarry is over the Combia stock in the south sector of the area, near 4.2 station, the extraction there is on a highly weathered profile, with the presence of an inverse fault that favours percolation of meteoric water into the rocks, with abundant oxides in the whole section outcropping. Soil uses are cattle raising at the lower elevations in terrains near of Arma river; agriculture is also an important activity especially near the locality of Damasco town, where big orange crops are covering big extensions of terrain.

4.3.4. Fluvial System

We compile a detailed geomorphological map of the fluvial system of the Arma river (Fig. 18). This map shows the Arma river valley from the eastern upstream zone of the study zone to the confluence with the Cauca river at the northwest side of the studied zone. Furthermore, this map displays the geomorphological expressions of the bars and aggradational terrace deposits.

Four river patterns are controlling the fluvial geomorphological system: straight, sinuous, meandered and anastomosed; sinuous pattern represents the prior form of the channel through its curse. River deposits consist of central and lateral bars and terraces, with ejection cones provided from tributaries. The objective behind describing river channel patterns is to understand the relationship between local focus zones of probable tectonic activity and changes in the channel patterns by the recognition of river zones where a meandering pattern changes to sinuosity along the river course, and where the river channel become straight with terraces bounding it (Burbank-Anderson, 2001).

First sinuous pattern of the river starts at the location of the unnamed fault east to Silvia-Pijao fault (Fig 18), that is controlling the river flow direction parallel to it, this sinuosity is developed next to the first pattern that appears on the section analyzed that is anastomosed; next to them, the river channel changes that tend and turn to the west, also becoming meandered due to the increase of sinuosity and that continue until it reaches a shuttered ridge associated to Silvia-Pijao fault; in this point, the river configuration turns straight and rapidly returns to meander, advancing some meters it gets straight again, with a lateral bar on the east side. These changes occur on the south of the Arma and Silvia-Pijao fault intersect, where the river encounters the third ejection cone present, this landform causes the river to redefine the flow direction, this effect left a meandering pattern, and make the river system to have a sinuous configuration above (Fig. 18).

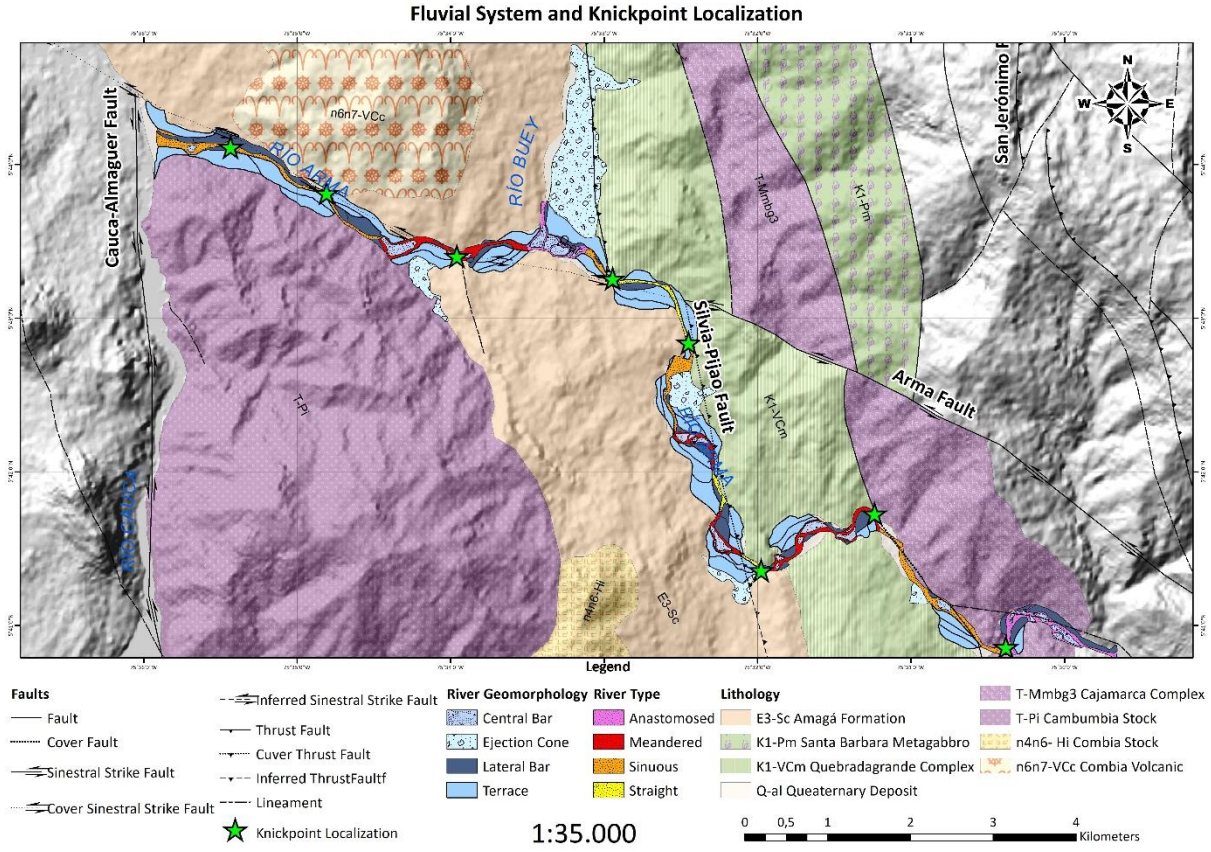

Figure 18. Fluvial system and knickpoints localization map link the river system pattern and the fluvial geomorphology.

At the intersection of the Silvia-Pijao fault and the Arma fault, a section of the river trend becomes straight and displays, first, the direction of Silvia-Pijao, then it changes to the Arma fault direction, with evidence of 2 lateral bar deposits on both sides and at least 4 terraces, 2 of that terraces, on the river eastern side at this point, are adjacent, suggesting two events of

aggradation. As the Arma fault system causes to the northern part of the Silvia-Pijao fault a displacement to the west, the valley seems to gets wider and the river became sinuous, then anastomosed, this change can be related with the presence of more and bigger sediments

added by the ejection cone that is formed in the Buey river mouth, into the Arma river.

Another meandered section appears after passing the ejection cone deposit associated with the Buey river, this continues until another ejection cone appears, and associated with the contact among the Amagá and the Cambumbia Stock, it causes the river pattern in front of it to reduce the meanders space and turn the river to sinuous. The biggest lateral bars are present in this zone, occupying the eastern side of the system and the formation of the terraces on its western side; the size and amount of these deposits can occur for being the nearest section to the Arma river mouth into Cauca river.

5. Discussion

Morpho-neotectonic studies on the zone allowed to stablish relations between landforms and the structural regime, specifically on the changes in patterns, terrace deposits and knickpoints along the Arma river channel, generated by the Arma fault and Romeral System fault intersections.

5.2. Structural

The study area corresponds to the intersection of sinistral NW-SE, dextral NE-SW and reverses N-S system faults. However, the movement of the blocks are independent between them (Fig. 12 &.19), blocks #1 and #4 slide towards NW along the reverse Silvia-Pijao fault and sinistral Arma fault, evidence an over-printing between NE-SW to NW-SE dextral kinematic. Block #2 turn clockwise between Arma and Cauca-Almaguer faults, shows a NE-SW sinistral-normal and NW-SE sinistral-reverse kinematic. Block #3 slide towards NW by the Silvia-Pijao fault and turn clockwise due to the Arma fault System, evidence NW-SE sinistral kinematic and NE-SW reverse. Block #5 slide towards SE through Arma fault System and below the Silvia-Pijao fault, indicate an NW-SE sinistral kinematic (Fig. 19).

According to our analysis, this section of the Cauca-Amagá valley behaves as a transpressional basin which the structural kinematics shows that the blocks on the west side of the Silvia-Pijao fault are displaced SE and clockwise, controlled by NW-SE sinistral faults, such as the Arma fault. While the blocks on the east side of the Silvia-Pijao fault are displaced NW and controlled by the N-S reverse faults such as the Romeral Fault System.

The paleo-stress and the joint analysis concludes that the NW-SE and NE-SW are the main stress tensors for the evolution of the valley, which agrees with the Peláez (2016) stress tensor evolution, that support a compressive tensor for an ENE-WSW Nazca subduction. For the

Jurassic to Cretaceous lithologies are not possible to determine a relative timing for their joint sets, due to that during Paleocene to Neogene the stress tensor changes twice between sinistral and dextral, overlapping the previous tectonic scenarios.

However, the Panama Choco Block collision and the ENE-WSW Nazca plate subduction reactivates the NW-SE sinistral, NE-SW dextral and N-S reverse kinematics simultaneously creating triple point jointly. Evident that the Silvia-Pijao and San Jerónimo fault displaces toward the east by the Arma fault, also the regional lineaments map (Fig. 20) shows an overlapping between all direction lineaments, particularly remarking a NE-SW trend.

The relationship between GIS and FD (Fig. 10.) shows a strong relationship among the lithology deterioration and the fault control over some part of the Cambumbia Stock, Cajamarca complex, Quebradagrande complex and Combia Stock. Additionally, few pieces of evidence over the Arma fault show a moderated weathering and moderated fault deterioration, remarking that the tropical environment and the tectonic dynamics overlap and erase the structural and lithological proofs. Finally, the anthropic alteration, such as quarries and infrastructure interventions, shows the best weathering and structural preservation conditions.

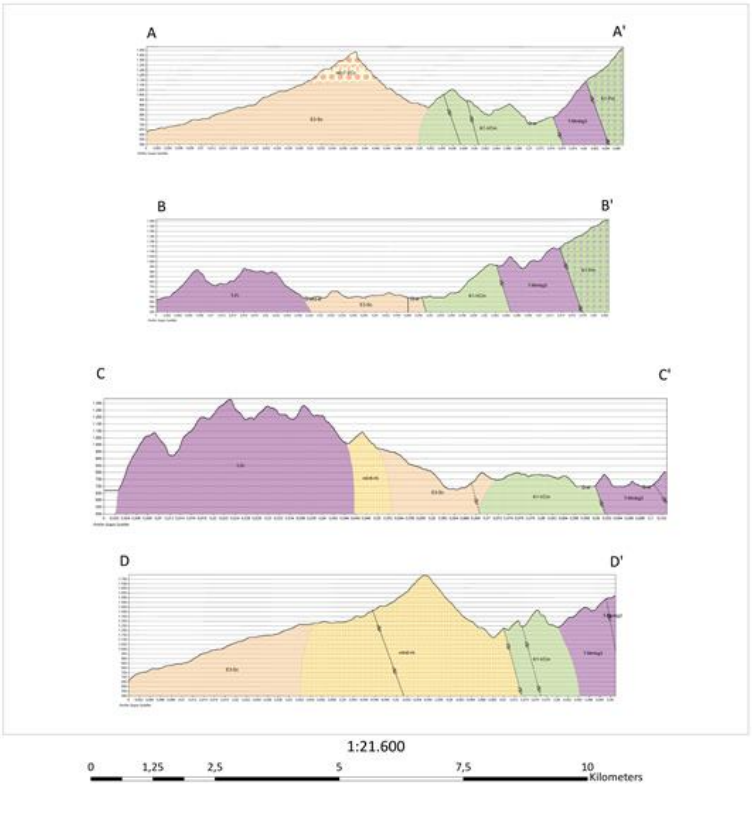

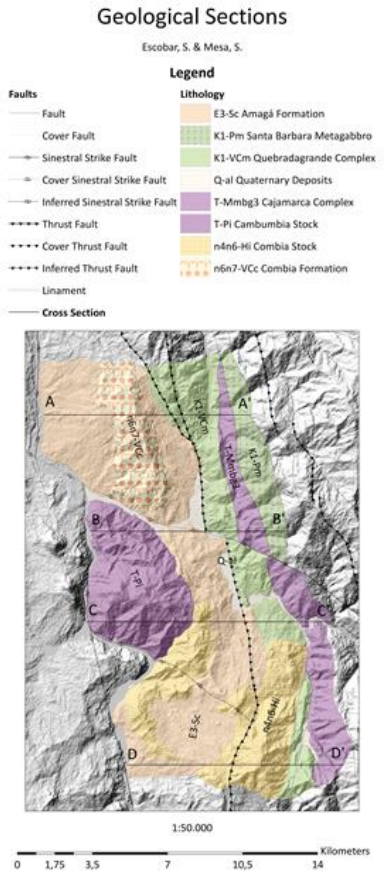

Figure 19. Geological sections. Interpretations of the current tectonic tensor of the study area.

5.2. Geomorphology

The study area is affected by the subduction of the Nazca plate, on the northern margin of the Cauca-Amagá valley, controlled by the Romeral and Arma fault systems intersection. The configuration and interaction between the structural blocks (Fig. 9), shows that at Buey river Basin sector, the tectonic geomorphology markers such as triangular facets and structural ridges are well exposed, also the landslides are controlled by the Romeral fault system.

On the western side of the Silvia-Pijao fault, the tectonic geomorphologic environment dominates the landscape with structural staggered slopes, on rocks of the Amagá Fm. Moreover, structurally degraded by the presence of NW-SE faults that behaviour as latitudinal limits between blocks #2 and #5; these slide towards SE through Arma Fault System and below the Silvia-Pijao fault with a clockwise kinematic (Fig. 18) this motion among them produce the structural ridges bending over by an NW-SE fault limit, also led expressions on triangular facets over the southern part of Cambumbia Stock, linked with the Cauca river change on its course direction.

The northwestern part is limited by the Arma fault at the southern border and the Silvia-Pijao fault on the east. This part shows morphologies controlled by the Amagá and Combia stratigraphy with a staggered to undulated hillsides, and denuded loins remarking the tributaries incision. Furthermore, the upper erosion scarps developed only on the Combia Fm.

The Arma fault controls the direction over the Arma river, until the Silvia-Pijao river's lineament, the river patterns of these section changes, initially by the knickpoint find at 11.2km, 12.4, 13.9km (downstream) (Fig. 20) relate to lithology's changes link to meandered to sinuous patterns. Secondly, the Buey River mouth contributes enough sediment to generate an anastomosed pattern, also in this section the degradational terraces start to evidence. Then, the intersection of the Arma fault with Silvia-Pijao fault system where is generated the second knickpoint zone and the river deposits shown two aggradational terrace events, possibly link with two different tectonic pulses. Between blocks #2, #3 and #4 show two different direction divide by the knickpoint found at 3.5km, the first direction present meandered, sinuous and straight patterns with 3 aggradational terraces event, produced by the Silvia-Pijao's reverse development. The second direction illustrates that the deposition space is closing towards the east until the knickpoint found at 2km, by this point the river becomes straight N-S trend. The Secas creek mouth represents where the degradational terraces increase the height difference with the Arma river, also upstream of this point the river patter change to anastomosed, suggesting that the straight pattern is related to an uplift of the N-S trend (Fig. 18).

6. Conclusions

We integrate structural geology with tectonic geomorphology analysis to evaluate the hypothesis of neotectonic activity along the Romeral fault system. Our analysis allowed us to conclude that neotectonic in the study area developed under a transpressive kinematic model, that produced compressive and distension stress tensor along the Arma fluvial system and a clockwise motion on the western structural blocks.

Furthermore, we can provide some final remarks about some specifics:

- The northern part of the Cauca-Amagá valley behaves as a transpressional basin which the structural dynamics shows that the blocks on the west side of the Silvia-Pijao fault displace SE and clockwise, controlled by NW-SE sinistral Arma System fault. While the blocks on the east side of the Silvia-Pijao fault displace NW controlled by the N-S reverse faults (Romeral Fault System).
- The ENE-WSW subduction of the Nazca plate reactivates the NW-SE sinestral, NE-SW dextral and N-S reverse kinematics simultaneously creating triple point joint, manifest in The Silvia-Pijao and San Jeronimo fault are displaced sinistrally by the Arma fault.
- The GIS and FD show a strong relationship among the lithology deterioration and the fault control, divided into 5 groups:
- 1 and 2 represent a well preserve blocky outcrop, related to the anthropologic intervention.
- 3 shows a less fracturing with middle weathering process.
- 4 and 5 both are controlled by the Romeral Fault System, however, the weathering intense depends on the distance of the faults.
- On the east of the Silvia-Pijao fault the tectonic landforms represent the low part of the western foothill landscape and predominate with the triangular facets which could be generated by secondary normal faults of the thrusting Romeral fault System.
- Blocks #2 and #5 clockwise kinematic produce that structural ridges bend over, also change the course direction of the Cauca river and an NW-SE sinistral fault that generates triangular facets over the southern part of Cambumbia Stock.
- The intersection of the Arma fault with Silvia-Pijao fault generated a knickpoint zone and the river deposits show two aggradational terrace events, possibly linked with two different tectonic pulses.
- The Silvia-Pijao fault river control produces a knickpoint and generates meandered, sinuous and straight patterns with three aggradational terraces events on this section of the Arma river.
- Degradational terraces show two groups limited by 700m elevation, the below group has a low angle slope and are closer to the aggradational terraces and colluvial deposits. The group above the 700m correspond to the south-eastern and higher part of the Arma river.

7. Recommendations

- Perform geophysics studies on the aggradational terraces to analyze the underground fault behaviour and the deposition behaviour.
- Perform geochronology cosmogenic studies in the ejection cones.
- To compile and to establish an integrated database of the seismic record of the Cauca-Amagá valley to collaborate with the Colombian seismic planning.
- Collect the history of satellite images over the study area to establish the landslide evolution.
- Complement the structural analysis on the northwestern part of the study area.

8. Cited References:

- Burbank, D.W., Anderson, R.S., 2001. Tectonic Geomorphology. Blackwell Science Ltd. 2, 13-33; 8, 159-175.
- Bürgl, H., 1967. The orogenesis in the andean system of colombia. Tectonophysics 4, 429-443.
- Bustamante, C., Archanjo, C.J., Cardona, A., Vervoort, J.D., 2016. Late Jurassic to Early Cretaceous plutonism in the Colombian Andes: A record of long term arc maturity. The Geological Society of America 172.
- Calle, B., González, H., De La Peña, R., Escorce, E., Durango, J., Ramíez, O., Alvarez, E., Calderón, M., Alvarez, J., Guarín, G. Rodríguez, C., Muñosz, J. Durán, J., 1980. Mapa Geológico de Colombia – Escala 1:100.000, Plancha 166 – Jericó: INGEOMINAS. Bogotá.
- Cardona, A., León, S., Jaramillo, J.S., Montes, C., Valencia, V., Vanegas, J., Bustamante, C., Echeverri, S. 2018. The Paleogene arcs of the northern Andes of Colombia and Panama: Insights on plate kinematic implications from new and existing geochemical, geochronological and isotopic data. Tectonophysics, 749, 88-103.
- Casas-Sainz, A.M., Gil-Peña, I., Simón-Gómez, J.L., 1990. Los métodos de análisis de paleoesfuerzos a partir de poblaciones de fallas: sistemática y técnicas de aplicación. Estudios geológicos 46, 385-398.
- Cediel, F., Shaw, R., Cáceres, C., 2003. Tectonic assembly of the Northern Andean block. In: Bartolini, C., Buffler, R., Blickwede, J. (Eds.), The Circum-Gulf of Mexico and the Caribbean: Hydrocarbon Habitats, Basin Formation and Plate Tectonics. American Association of Petroleum Geologists Memoir 79, 815–848.
- Chicangana, G., 2005. The Romeral fault system: a shear and deformed extinct subduction zone between oceanic and continental lithospheres in northwestern South America: Earth Sciences Research Journal 9, 51 – 66.
- Delvaux, D., 2010. Win-Tensor User Guide: PBT Module.
- Delvaux, D., 2012. Release of program Win-Tensor 4.0 for tectonic stress inversion: statistical expression of stress parameters. Geophysical Research Abstracts 14.
- Delvaux, D., Sperner, B., 2003. New aspects of tectonic stress inversion with reference to the TENSOR program. Geological Society Special Publication 212, 75-100.
- Doornkamp, J. C., 1986. Geomorphological approaches to the study of neotectonics. Journal - Geological Society (London) 143, 335-342.
- Ego, F., Sébrier, M., Yepes, H., 1995. Is the Cauca – Patía and Romeral Fault System Left or Rightlateral. Geophysical Research Letters 22, 33-36.
- Gomez, J., Nivia, A., Montes, N.E., Jiménez, D.M., Tejada, M.L., Sepúlveda, M.J., Osorio, J.A., Gaona, T., Diederix, H., Uribe, H Mora, M., 2007. Compiladores. Mapa Geológico de Colombia. Escala: 1:1´000.000. Ingeominas, Bogotá.
- Hoek, E., Brown, E.T., 2019. The Hoek–Brown failure criterion and GSI – 2018 edition. Journal of Rock Mechanics and Geotechnical Engineering 11, 445-463.
- Hong, K., Han, E., Kang, K., 2017. Determination of geological strength index of jointed rock mass based on image processing. Journal of Rock Mechanics and Geotechnical Engineering 9, 702-708.

- Jaramillo, J.S., Cardona, A., León, S., Valencia, V., Vinasco, C., 2017. Geochemistry and geochronology from Cretaceous magmatic and sedimentary rocks at 6°35′ N, western flank of the Central cordillera (Colombian Andes): Magmatic record of arc growth and collision. Journal of South American Earth Sciences 76, 460-481.
- Jaramillo, J.S., Cardona, A. Monsalve, G., Valencia, V., Leon, S. 2019. Petrogenesis of the late Miocene Combia volcanic complex, northwestern Colombian Andes: Tectonic implication of short term and compositionally heterogeneous arc magmatism. Lithos 331, 194-210.
- Kulatilake, P.H.S.W., Fiedler, R., Panda, B.B., 1997. Box fractal dimension as a measure of statistical homogeneity of jointed rock masses. Engineering Geology 48, 217-229.
- Lara, M., Salazar-Franco, A.M., Silva-Tamayo, J.C., 2018. Provenance of the Cenozoic siliciclastic intramontane Amagá Formation: Implications for the early Miocene collision between Central and South America. Sedimentary Geology 373, 147-162.
- López, C., Mario, M.S., Franck A., Audemard, M., 2009. Deformación Tectónica Reciente En Los Pie De Montes De Las Cordilleras Central Y Occidental, Valle Del Cauca, Colombia. Boletín de Geología 31, 11-29.
- MacDonald, W.D., Estrada, J.J., Sierra, G.M, Gonzales, H. 1996. Late Cenozoic tectonics and paleomagnetism of North Cauca Basin intrusions, Colombian Andes: Dual rotation modes. Tectonophysis 261, 277-289.
- Meschede, M., Barckausen, U., 2000. Plate tectonic evolution of the Cocos–Nazca spreading center. In: Silver EA, Kimura G, Shipley TH (eds) Proceedings of the ocean drilling program, scientific results. A.M. University 170, 1–10.
- Montgomery, D.R., Balco, G., Willett, S.D., 2001. Climate, tectonics, and the morphology of the Andes. Geology 29, 579-582.
- Moreno, M., Pardo, A., 2003. Stratigraphical and sedimentological constraints on Western Colombia: implications on the evolution of the Caribbean plate. In: Bartolini C, Buffler RT, Blickwede, J (eds) The Circum-Gulf of Mexico and the Caribbean: Hydrocarbon habitats, basin formation, and plate tectonics. American Association of Petroleum Geologists Memoir 79, 891–924.
- Nivia, A., Marriner, G.F., Kerr, A.C., Tarney, J., 2006. The Quebradagrande Complex: A Lower Cretaceous ensialic marginal basin in the Central Cordillera of the Colombian Andes. Journal of South American Earth Sciences 21, 423-436.
- Noriega-Londoño, S., Restrepo-Moreno, S.A., Vinasco, C., Bermúdez, M.A., Min, K., 2019. Thermochronologic and geomorphometric constraints on the Cenozoic landscape evolution of the Northern Andes: Northwestern Central Cordillera, Colombia. Geomorphology 351.
- Panizza, M., Castaldini, D., Bollettinari, G., Sassari, A., Carton, A.,1987. Neotectonic research in applied geomorphological studies. Zeitschrift fur Geomorphologie, Supplementband 63, 173-211.
- Pelaez Z.E., 2016. Obtención De Paleoesfuerzos Del Sistema De Fallas Cauca - Romeral En El Sector Norte De La Cuenca Amagá, Entre Las Localidades De Titiribí Y Quebrada Sinifaná. Escuela de ciencias departamento de geología Universidad EAFIT.
- Piedrahita, V.A., Bernet, M., Chadima, M., Sierra, G.M., Marín-Cerón, M.I., Toro, G. E., 2017. Detrital zircon fission-track thermochronology and magnetic fabric of the Amagá Formation (Colombia): Intracontinental deformation and exhumation events in the northwestern Andes. Sedimentary Geology 356, 26-42.

- Ramirez-Arias, J.C., Mora, A., Rubiano, J. Duddy, I., Parra, M., Moreno, N., Stockli, D., Casallas, W., 2012. The asymmetric evolution of the Colombian Eastern Cordillera. Tectonic inheritance or climatic forcing? New evidence from thermochronology and sedimentology. Journal of South American Earth Sciences 39, 112-137.
- Ratzov, G., Sasson, M., Collot, J.Y., Migeon, S. 2012. Late Quaternary geomorphologic evolution of submarine canyons as a marker of active deformation on convergent margins: The example of the South Colombian margin. Marine Geology 315-318, 77-97.

- Salcedo, E., Pérez, J.L. 2017. Deformación sismotectónica a partir de mecanismos focales de terremotos en el Valle del Cauca, suroccidente de Colombia. Revista Geológica de América Central 57, 23-43.
- Schillaci, C., Braun, A., Kropáček, J., 2015. Terrain analysis and landform recognition. Department of Geosciences, Tuebingen University, Germany.
- Silva-Tamayo, J.C., Sierra, G.M., Correa, L.G., 2008. Tectonic and climate driven fluctuations in the stratigraphic base level of a Cenozoic continental coal basin, northwestern Andes. Journal of South American Earth Sciences 26, 369-382.
- Spikings, R., Cochrane, D., Villagomez, D., Van der Lelij, R., Vallejo, C., Winker, W., Beate, B. 2015. The geological history of northwestern South America: From Pangaea to the early collision of the Caribbean Large Igneous Province (290-75 Ma). Gondwana Research 27, 95-139.
- Suter, F., Martínez, J.I., Vélez, M.I. 2011. Holocene soft-sediment deformation of the Santa Fe-Sopetrán Basin, northern Colombian Andes: Evidence for pre-Hispanic seismic activity. Sedimentary Geology 235, 188-199.
- Suter, F., Sartori, M., Neuwerth, R., Gorin, G. 2008. Structural imprints at the front of the Chocó-Panamá indenter: Field data from the North Cauca Valley Basin, Central Colombia. Tectonophysics 460, 134-157.
- Taboada, A., Rivera, L., Fuenzalida, A., Cisternas, A., Phillip, H., Bijwaard, H., Olaya, J., Rivera, C., 2000. Geodynamics of the northern Andes: subductions and intra- continental deformation (Colombia). Tectonics 19, 787–813
- Vinasco, C., 2019. The Romeral Shear Zone: The Pacific-Caribbean-Andean Junction. Geology and Tectonics of Northwestern South America.
- Vinasco, C., Cordani, U., 2012. Episodios De Reactivación Del Sistema De Fallas De Romeral En La Parte Nor-Occidental De Los Andes Centrales De Colombia a Través De Resultados 39Ar-40Ar Y K-Ar. Boletín Ciencias de la Tierra 32, 111-124.
- Žalohar, J., Vrabec, M., 2008. Combined kinematic and paleostress analysis of fault-slip data: The Multiple-slip method. Journal of Structural Geology 30, 1603-1613.
- Zapata, S., Cardona, A., Jaramillo, J.S., Patiño, A., Valencia, V., Leon, S., Mejia, D., Pardo-Trujillo, A., Castañeda, J.P. 2018. Cretaceous extensional and compressional tectonics in the Northwestern Andes, prior to the collision with the Caribbean oceanic plateau. Gondwana Research journal 66, 207-226.